NTNU

Norwegian University of
Science and Technology

Autonomous Algorithms for Dynamic Spectrum Management in DSL Systems

Jan Vidar Rognsvåg

Master of Science in Communication Technology
Submission date: June 2008
Supervisor: Nils Holte, IET

Norwegian University of Science and Technology
Department of Electronics and Telecommunications

Problem Description

I dagens standarder for DSL (Digital Subscriber Lines) er det satt maksimalverdier for utsendt effekttetthet i ulike frekvensområder. Kompatibiliteten mellom DSL systemene ivaretas ved at alle brukere ligger innenfor disse maksimalverdier. Dette gjør at dimensjonering av systemene må baseres på verste tilfelle av interferens, noe som fører til relativt pessimistiske estimater for rekkevidder og bitrater.

Det arbeides internasjonalt med å ta i bruk en dynamisk frekvensbruk i DSL systemer (DSM - Dynamic Spectrum Management) for å oppnå økt ytelse. Denne oppgaven skal ta for seg den enkleste formen for DSM som består av autonome DSL systemer som automatisk minimaliserer utsendt spektrum i eget transmisjonssystem basert på iterativ "water-filling".

Assignment given: 14. January 2008
Supervisor: Nils Holte, IET

ABSTRACT

Interfering crosstalk from adjacent twisted pairs has become the dominant source for performance degradation in Digital Subscriber Line (DSL) systems. In present systems a Static Spectrum Management (SSM) is performed with no considerations for frequency dependencies in the interfering noise spectrum and channel attenuation. A dynamic power allocation is introduced in the research field Dynamic Spectrum Management (DSM) to significantly reduce the crosstalk interference.

This report evaluates the development- and examines the advantages of autonomous algorithms for distributed power control, thus avoiding demands of centralized coordination and terminal hardware upgrades as required for more complex algorithms in DSM. Hence, this thesis presents algorithms for cost-effective implementation in present twisted pair broadband communication. Most implemented algorithms performed well above the capacities at SSM. The best results were however achieved by the iterative water-filling algorithm and in particular for an interference impaired subscriber in a three-user environment where it achieved near twice the rate compared to SSM. The iterative water-filling algorithm was correspondingly applied to a full binder of ten pairs with statistical coupling based on empirical research. However, this approach led to less impressive results than in the three-user environment. None the less, distributed algorithms in digital subscriber lines appear to be a good investment as an incremental step in broadband communication. The implementation of autonomous algorithms for dynamic spectrum management will also favour the advancement of more complex algorithms of DSM in the bid to revolutionize the bit rates of twisted copper pairs.

PREFACE

This thesis was completed at the Norwegian University of Science and Technology (NTNU), Faculty of Information Technology, Mathematics and Electrical Engineering (IME), Department of Electronics and Telecommunications (IET). The report is part of the subject TFE4900 – Signal Processing and Communication which was the final fulfilment for obtaining a Masters' Degree in Communication Technology at NTNU in spring 2008.

I would like to thank Professor Nils Holte at IET for his contributions as supervisor and specialist in affiliation to this thesis and also for his guidance and motivation during my masters' degree at NTNU. Secondly I would like to thank Professor John M. Cioffi at Stanford University for further inspiration and for giving access to some of his own research on the subject. I would also like to thank associate Professor Lars Lundheim at IET for his constructive feedback while concluding this report.

Trondheim 23. June 2008

Jan Vidar Rognsvåg

CONTENTS

LIST OF FIGURES

LIST OF TABLES

ABBREVIATIONS

ADSL	Asymmetric DSL: Asymmetric bit rates with more capacity in the downstream transmission
ASB	Autonomous Spectrum Balancing: Algorithm for a near optimal spectrum balancing in DSM level 1
BER	Bit Error Rate/Ratio: Probability for error in receiving a bit
CAP	Carrierless Amplitude/Phase modulation
CO	Central Office
CP	Customer Premises
DAIM	NTNU's digital archives for submitted master thesis
DLM	Dynamic Line Management: Analogy to DSM level 1
DMT	Discrete Multi-Tone Modulation: Dividing the frequency band in carriers/tones
DSL	Digital Subscriber Lines: High speed digital communication on regular cobber lines
DSLAM	DSL Access Multiplexing
DSM	Dynamic Spectrum Management: Permitting variations in the transmit PSD
FDD	Frequency-Division Duplexing: Up- and downstream communication in separate frequency bands
FEXT	Far-End Crosstalk: Electromagnetic coupling originating from TX in opposite end of comm. system
FSAN	Full Service Access Network: Interest group for the world's leading telecom services providers
FTTH	Fibre To The Home: Fibre cabling all the way till the CP
HFC	Hybrid Fibre-Coaxial: Transmission using both fibre and twisted cobber pairs
ISB	Iterative Spectrum Balancing: Algorithm for a near optimal spectrum balancing on DSM level 2
ITU	International Telecommunication Union
IWF	Iterative water-filling: Algorithm for distributed spectrum allocation in DSM level 1
MIMO	Multiple Input Multiple Output: Bonding multiple channels for increased throughput
NEXT	Near-End Crosstalk: Electromagnetic coupling originating from TX in same end of comm. system
OFDM	Orthogonal Frequency-Division Multiplexing
OSB	Optimal Spectrum Balancing: Algorithm for a near optimal spectrum balancing on DSM level 2
PAR	Peak-to-Average Ratio
POTS	Plain Old Telephone Service
PSD	Power Spectral Density
PSTN	Public Switched Telephone Network: Official description of POTS
PVC	Polyvinylchloride: Thermoplastic polymer used in shielding the cobber cables
RT	Remote Terminal
RX	Receiver in a communication system
SDD	Space Division Duplexing: Up- and downstream communication in separate cables (dual simplex)
SMC	Spectrum Maintenance Centre/ Spectrum Management Centre: Centralized spectrum coordination
SNR	Signal-to-Noise Ratio
SSM	Static Spectrum Management: Equal transmitted PSD for all carriers
TDD	Time Division Duplexing: Up- and downstream communication separated in time intervals
TX	Transmitter in a communication system
VDSL	Very high bit rate DSL: Limited at 52 Mbps in the downstream direction

1. Introduction

1.1. Background

Digital Subscriber Lines has become the standard technology for broadband communication and had by the end of 2006 an approximated 185 million subscribers worldwide. The prosperity of virtually unlimited bit rates in fibre communication has however increased the demands for higher bit rates also in DSL. The interference from other lines that share the same telephone cable binder is usually the constraint for achieving higher bit rates. This interference is denoted crosstalk and has become the main obstacle for the advancement of DSL technology. However, as DSL has the economical advantage of using existing copper lines in the telephone infrastructure, fibre cabling is expensive in both production and installation. Extensive research is thus dedicated to the subject denoted Dynamic Spectrum Management (DSM) with the T1E1.4 working group and the IEEE 802 working group both as substantial contributors. In contrast to Static Spectrum Management (SSM) which assumes a worst case scenario of the interference for all subscribers in the binder, DSM technology will allow modems to measure interference and transfer functions before transmitting its spectrum. Hence, distributed algorithms let the modems eliminate redundant transmitted power which exceeds what is needed for customers' bit rates. The least complex algorithms for dynamic spectrum allocation increase the spectrum density in lightly interfered carriers in multi carrier modulation, consequently increasing these carriers' signal-to-noise ratio. Heavily interfered carriers receive less spectral density and for the worst cases of interference where no bits can be transmitted, they are shut off completely. These algorithms can conveniently be implemented with mere software upgrades to the modems, reducing implementation costs to a minimum.

1.2. Objectives

The objective of this thesis is to analyze the well known iterative water-filling algorithm (IWF), implement it in MATLAB® programs and compare the performance to static spectrum management. Further algorithms for dynamic spectrum allocation were then to be analyzed and implemented for comparison with both SSM and the IWF. All algorithms were to be applicable to present DSL technology for uncomplicated implementation in twisted copper pair communication. Descriptions of the advantages and limitations were given for each algorithm

1.3. Limitations

Crosstalk is categorized based on the location of the interfering transmitter in contrast to the interfered receiver and denoted as near-end crosstalk and far-end crosstalk, both described in Chapter 2.1. This report focuses however mainly on far-end crosstalk, thus near-end crosstalk is eliminated from the calculations as justified in Chapter 2.1.1. DSM is categorized in three levels defined by an increase in algorithm complexity and system implementation costs with consecutive reduction of interfering crosstalk and increase in capacity. The three levels of DSM consist of autonomous power distribution at level 1 as mentioned in the first section, centralized spectrum measuring and distribution at DSM level 2 and vectoring and bonding between different DSL lines at level 3. The more advanced algorithms of DSM level 2 and 3 need centralized coordination from a Spectrum Maintenance Centre (SMC) which introduces demands of hardware upgrades. The main subject for research in this report is DSM at level 1, thus DSM at level 2 and 3 will only briefly be presented in Chapter 2.3.

1.4. Outline

In Chapter 2 there will be given a concise presentation of crosstalk interference and dynamic spectrum management in particular. The chapter also offers a preamble to the results with a description of the system and its parameters. The actual calculations, which are the main focus area of this report, is presented in Chapter 3 and successively discussed in Chapter 4. Finally, there will be given a brief conclusion to the thesis and its calculations in Chapter 5. The Vancouver reference model is applied with references to specific page number for quotation.

2. Spectrum Management

2.1. Interference

The last stretch of a DSL communication system is build up of pairs of copper conductors insulated with PVC and twisted to reduce emanating electromagnetic radiation. When interfering on other pairs in the same binder this radiation is denoted *crosstalk* and is one of the biggest impairments on DSL systems today. A binder normally consists of 10 to 50 pairs, again bundled together in cables of up to 2000 pairs [1]. The cable can deliver broadband communication to equally many customers in last mile communication between the central office (CO) and the customer. This distance is often in reality only a few hundreds of meters since fibre cabling constantly reach closer towards the customer premises in present hybrid fibre-coaxial (HFC) networks illustrated in Figure 1. Attenuation is a declining problem for these short distances and interference becomes the decisive impairment to the capacity of the transmission system. Sources of interference like impulse interference, interference from radio frequencies and white noise are all disturbing factors; however crosstalk coupling between twisted pairs within the same binder is typically the dominant source of performance degradation [2]. Crosstalk interference was previously significant in the Public Switched Telephone Network (PSTN), also known as the "Plain Old Telephone Service" (POTS), and made it possible to listen in on neighbors' conversations with telephone equipment connected through the same binder. Crosstalk is no longer a problem in PSTN, but significantly reduces the signal-to-noise ratio (SNR) of a high frequency communication channel. Crosstalk is further categorized in near-end crosstalk and far-end crosstalk, which both will be discussed in the following section. The red lines denoted crosstalk in Figure 1 corresponds to the second category. RT is an abbreviation for *remote terminal* used to connect subscribers farther away from the central office. DMT transmission will be discussed in Chapter 2.2.

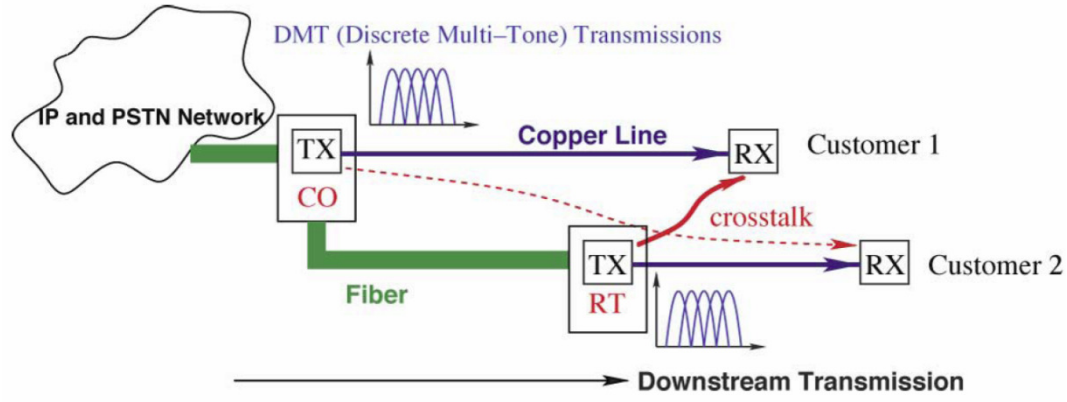

Figure 1: Important parts in Hybrid Fibre-Coaxial Communication [3].

2.1.1. Near-End Crosstalk

Near-end crosstalk (NEXT) is the electromagnetic coupling between two twisted pairs generated from a transmitter- and disturbing a receiver in the same end of a communication system. This interference will thus not be attenuated by the channel and NEXT is thus often the decisive impairment in DSL systems with co-located transmitters and receivers operating on the same bandwidth. The "simplified NEXT model" which is a simplification of the Unger model [5] denotes the one percent worst case coupling loss between two twisted pairs in the same binder and is given in (1):

$$|H_{NEXT}(f,N)|^2 = K_{NEXT} N^{0.6} f^{3/2} \quad (1)$$

N is the number of disturbing users, K_{NEXT} is a proportionality constant and f is the frequency of the carrier. The one percent worst case coupling loss implies only one percent of the tested twisted pairs experience greater loss, i.e. less interference, of the interfering power of the disturbing twisted pair. NEXT cancellation is performed by dividing the channel bandwidth in upstream- and downstream channels with Frequency-Division Duplexing (FDD) with simple bandpass filtering to remove the interfering frequency components. NEXT can also be avoided with Time Division Duplexing (TDD) where the channel is split in time intervals letting the CO and the subscriber access the channel in different periods [4]. Another possibility includes four-wire duplexing, which in reality is a dual-simplex since the communication is split in two different twisted pairs for upstream- and downstream communication. Hence, this type of duplexing is also defined as Space Division Duplexing (SDD). Effective line codes are also used where in particular the code 2B1Q could be mentioned. As the name implies, 2B1Q codes two binary digits into one quaternary symbol. Because of its efficient treatment of near-end crosstalk and intersymbol interference the code has been adopted as the North-American standard for digital subscriber loops [6]. NEXT is further categorized in self- and alien NEXT. Self NEXT is the near-end crosstalk from other similar systems within the binder while alien NEXT is the near-end crosstalk from dissimilar transmission systems in overlapping frequency bands in the same binder.

2.1.2. Far-End Crosstalk

In contradiction to NEXT, far-end crosstalk (FEXT) is the coupling between transmitters and receivers in the opposite ends of the cable, i.e. transmitted power in a twisted pair induces a power also in adjacent twisted pairs with signals travelling in the same direction. Similar to the NEXT model, an expression is also given for the one percent worst case FEXT coupling between two twisted pairs [5];

$$|H_{FEXT}(f, L, N)|^2 = K_{FEXT} N^{0.6} L f^2 |H_{channel}(f, L)|^2, \quad (2)$$

where N, K_{FEXT} and f is the number of disturbing users, the proportionality constant and the frequency respectively, as in (1). L is the channel's loop length while $H_{channel}(f, L)$ is the voltage transfer function of the channel from the transmitter of the interfering signal to the interfered receiver. The coupling effect is especially unfortunate at high frequencies and thus a big problem in present DSL systems where higher frequency bands are used to expand the bandwidth. Far end crosstalk is also proportional to the joint cable length and will have more effect on systems where two twisted pairs follow the same binder for a longer distance. Similar to the NEXT model in (1) also the FEXT model in (2) is based on the one percent worst case crosstalk coupling and gives a pessimistic analysis for multi-user environments. Studies by the Full Service Access Network group (FSAN) [7] indicate a more realistic approach of adding up the power contributions from different crosstalk sources:

$$FE_{tot} = (FE_1^{1/0.6} + FE_2^{1/0.6})^{0.6} \quad (3)$$

FE_1 and FE_2 are here the interference power allocation in two different twisted pairs interfering on a third twisted pair with the total power allocation of FE_{tot}. This is an empirical model and the reason for the exponential in the expression is explained to have no physical justification, but an origin from research on North American cabling [8]. This model has been given broad acceptance and simulations show a lower error estimate when comparing to former proposals. The calculations in this report has the objective to verify empirical models as in (3) better represent the real crosstalk interference than the worst case coupling assumptions as implemented in present DSL systems. In reality the crosstalk coupling differ for all twisted pair relations in a binder and will in this thesis be applied with both fixed and statistical values. FEXT is furthermore divided in self- and alien FEXT where alien FEXT is the coupling from different transmission systems within the same cable as described for NEXT. This study is devoted to self far-end crosstalk which thus will often be denoted merely as *crosstalk*.

2.1.3. **Near-Far Problem**

An important aspect when designing DSL systems are the locations of its terminals in the loop environment. A transmit signal entering a binder where other signals already has received significant attenuation could introduce decisive interference on the other lines' signal. An illustration of this concept in the downstream case is presented in Figure 2 denoted the near-far problem: The RT's transmit power will cause significant crosstalk to user 1's receiver, denoted RX_1, and severely limit this user's signal-to-noise ratio. The CO transmitter

denoted TX_1 will introduce little interference to the second customer's receiver; RX_2, due to the significant attenuation of the signal prior to interfering on the second line.

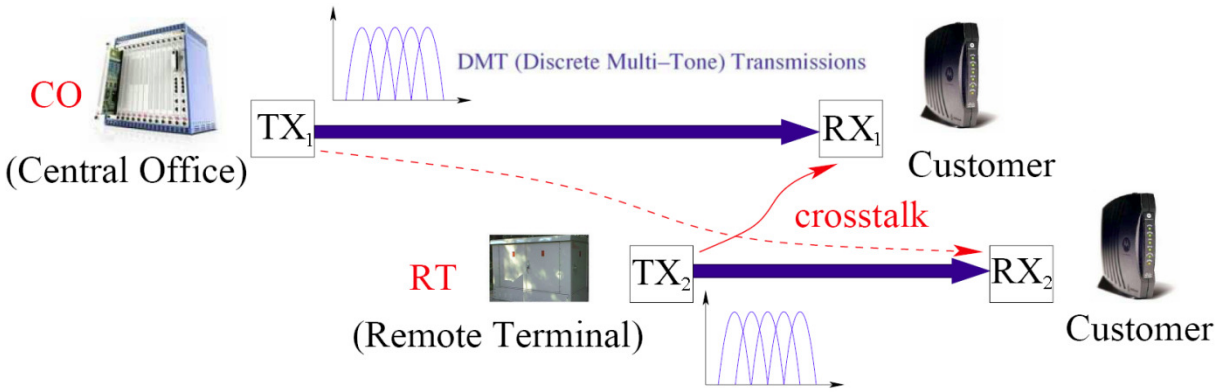

Figure 2: Near-Far problem in downstream communication [9]

The RT introduces a significant interference in the already attenuated signal transmitted from TX_1.

In the upstream channel's similar scenario of Figure 3, widely spread subscribers, both close to the CO and far away from the CO, introduce similar crosstalk coupling as the CO- and RT transmitters of Figure 2. A signal originating from the first users transmitter; TX_1, will add limited interference to the received signal in RX_2. However the signal originating from TX_1 could add severe interference to the received signal in RX_2 and thus be the decisive impairment of the SNR for the first customer's upstream transmission to the CO. The Near-Far problem introduces decisive performance degradation in present DSL communication with RTs and customers all along the loop environment.

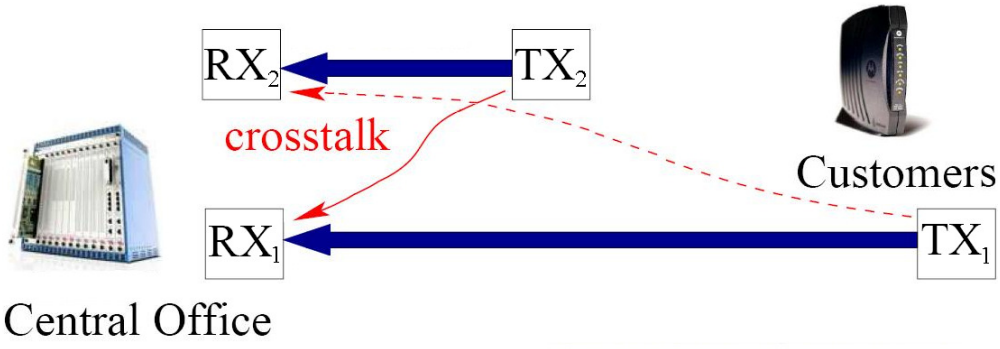

Figure 3: Near-Far problem in upstream communication

Transmit power from a customer close to the CO will generate a dominant interfering crosstalk on the signal transmitted from customers farther away.

2.2.Discrete Multi-Tone Modulation

Discrete Multi-Tone modulation (DMT) was included in ITU G.992.1 [10] in 1999, succeeding the former standard known as Carrierless Amplitude/Phase modulation (CAP), and divides the bandwidth in carriers or "tones" based on orthogonal frequency-division multiplexing (OFDM). Each carrier can be regarded as an autonomous transmission channel,

which makes specific signal constellations for each separate carrier feasible, and is thus often denoted Multi Carrier Modulation (MCM) [11]. DMT has in particular increased flexibility of DSL systems with the ability to configure the spectrum and the bit loading in accordance to the noise conditions in the system. Interference light carriers can thus transmit with increased bit rate, whereas carriers with a low SNR only has few bits loaded to its channel. Hence the total transmitted power in the twisted pair is reduced. Transmitting the spare power in carefully chosen carriers implies a capacity increase compared to bit loading techniques with an equal signal constellation in every carrier. The bit loading is given by the signal-to-noise ratio in each separate carrier [12]:

$$b_n(k) = log_2\left(1 + \frac{SNR_n(k)}{\Gamma_n}\right) \quad (4)$$

Here *k* refers to the carrier index while *n* is the n'th user in a multiuser environment. $SNR_n(k)$ is the signal-to-noise ratio of user n and carrier k. Γ_n is a constant reflecting the Shannon gap and can be viewed as the degradation in performance of real systems relative to the theoretically optimal Shannon performance [13 p. 111]. Deriving the expression for the signal-to-noise ratio in a two-user environment results in the following formula, here presented for user 1 [12]:

$$b_1(k) = log_2\left(1 + \frac{|H_{11}(k)|^2 P_1(k)}{\Gamma_1(|H_{12}(k)|^2 P_2(k) + N_1(k))}\right) \quad (5)$$

$H_{11}(k)$ is the transfer function for the attenuation channel at carrier k, while $H_{12}(k)$ is the transfer function for the crosstalk channel from the interfering transmitter of the second user to the receiver of the first user. $P_1(k)$ and $P_2(k)$ are the transmitted power in carrier k for signal 1 and 2 respectively and finally; $N_1(k)$ describes the total noise power different from self FEXT at carrier k for user 1. Figure 4 illustrates the transfer functions in the frequency domain of the attenuation channels denoted $H_{11}(f)$ and $H_{22}(f)$ and the crosstalk coupling functions denoted $H_{12}(f)$ and $H_{21}(f)$. $S_1(f)$ and $S_2(f)$ are the transmitted spectrums of the two users and thus have the following relation to $P_n(k)$:

$$P_n(k) = \int_{FL+k\cdot W_c}^{FL+(k+1)W_c} S_n(f)\, dF \quad (6)$$

FL is the lower bound of the system bandwidth while W_c is the carrier bandwidth. Similar equation for the carrier noise power $N_n(k)$ is given in (7):

$$N_n(k) = \int_{FL+kdW}^{FL+(k+1)dW} N_n(f)\, dF \quad (7)$$

$N_n(f)$ is the total noise spectrum of all interfering noises excluding the far-end crosstalk.

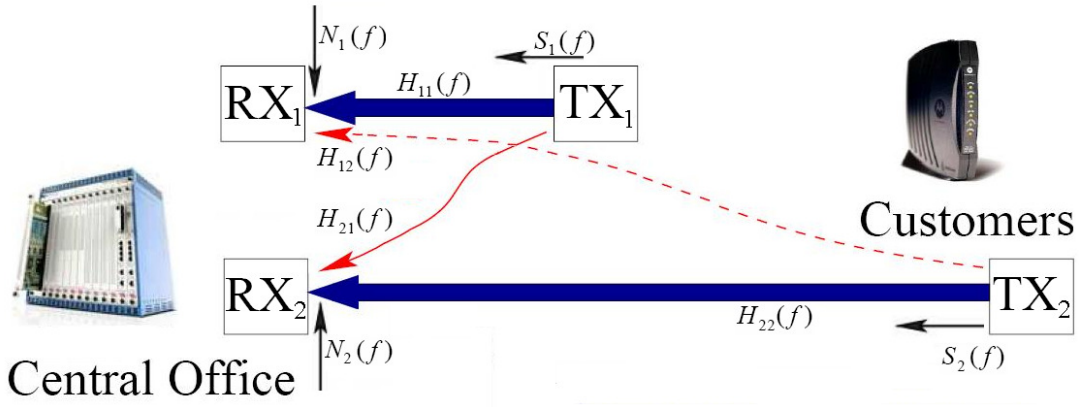

Figure 4: Transfer functions in DSL

Illustration of a two-user environment with its transfer functions for both the attenuation and the crosstalk channel in upstream communication.

The transfer functions denoted $H(f)$ in the figure will be further described in Chapter 2.5. While modems formerly have been operated in two different modes; Margin Adaptive mode and Rate Adaptive mode, DMT permits the implementation of a third mode denoted Power Adaptive mode. Margin adaptive mode is however the most common in DSL modems today and uses all available power to maximize the noise margin which is included in the Shannon gap denoted Γ in (4). An increase in the noise margin decreases the probability of receiving a bit other than the transmitted bit and thus decreases the bit error rate (BER). The transmission rates will thus remain unchanged for all signal-to-noise ratios exceeding a minimum noise margin. Rate Adaptive mode also uses all available power but specifies a fixed margin to maximize the signal-to-noise ratio and thus also the capacity. The third alternative is the mentioned Power Adaptive mode also known as the "Fixed Margin" mode, which specifies a fixed margin and eliminates all excessive power spectral density (PSD) in the SNR where this margin is superseded. Consequently, only the power required to maintain a predefined bit rate is transmitted, ensuring a fixed bit rate for any SNR above the given minimum value. This mode is easily implemented by a flat power back-off (PBO) to minimize the power transmitted from modems in short loops where excessive power contribute to interfering crosstalk constraining the capacity in adjacent systems. This relatively new method for power control is proposed to be implemented in all DSL transceivers because of its superior characteristics against crosstalk. Further proposals include abandoning the principle of spectral masks constraining the power spectral density. Hence, modems would gain the ability of "boosting" the spectrum in frequency bands with a low level of interference where no other signal might be present [12]. The different operating modes are presented in Table 1 with a description of their feature at high signal-to-noise ratios:

Table 1: Different modes for operating a modem:

Margin Adaptive Mode	Increase noise margin
Rate Adaptive Mode	Increase transmission bit rate
Power Adaptive Mode	Reduce power to reduce crosstalk interference

2.3.Dynamic Spectrum Management

Spectrum management has earlier only been given modest acknowledgement in digital subscriber line networks in contrast to the vast research on the topic today. In present systems a static spectrum management (SSM) has been applied, initially designed for single user systems. The transmit power spectral density has been set to a fixed level for all modems regardless of how the subscribers and terminals are located in the loop environment [14]. This worst case allocation procedure has previously been adequate since crosstalk for lower bit rates and frequencies rarely is the decisive impairment. However, with the high bit rate transmission in short distance communication, as the prosperous VDSL standard, crosstalk has been shown to be the most significant interference and in general 10 dB to 15 dB more powerful than the background noise [15]. SSM will in these systems lead to pessimistic assumptions of the crosstalk from long lines since these are assumed to contribute with as much interference as the shortest lines. Thus an unnecessary low PSD will be allocated to most of the transmitters, limiting the total bit rate significantly. Adaptive allocation of the power spectra for each modem based on the physical location of the transmitting- and receiving modems together with an analysis of the channel characteristics, will however radically improve the exploitation of the capacity in twisted pair cables. A joint optimization of the binder's transmitted power is achieved while limiting the crosstalk and increasing the achievable bit rates. This form of power allocation is denoted Dynamic Spectrum Management (DSM). DSM is categorized in three different levels with increasing complexity of the algorithms and implementation for each level. SSM, which falls outside the definition of dynamic spectrum management, is identified as a level zero DSM. At DSM level 1 there are only incremental changes to the technology to ensure compatibility with existing technology and modem hardware [16]. Each subscriber line is regarded as an autonomous channel and all management is thus performed in a distributed manner. DSM at level one is thus often denoted Dynamic Line Management (DLM). This implies there is no coordination between the lines, but only an optimization of each specific line's power allocation to minimize emanating electromagnetic radiation denoted crosstalk coupling. The most straightforward approach of DLM is to prevent what Cioffi [17] labels as "hogging". Hogging

occurs when transmit power in a modem gives rise to crosstalk causing severe interferences and dominating all other lines in the same binder, e.g. the near-far problem. In DSM the modems are instead set to practice a "polite" access to the medium. Merely power necessary to maintain a specified bit rate is transmitted, consequently eliminating redundant interference on adjacent subscriber lines equivalent to the previously introduced power adaptive mode in Chapter 2.2. Two different algorithms for dynamic line management are the near-optimal method denoted Autonomous Spectrum Balancing (ASB) [3] and the Iterative Water-Filling (IWF) algorithm presented in Chapter 2.4. The left part of Figure 5 illustrates water-filling with excessive power spectrum density S(f), consequently hogging all the resources in the respective binder. The right part of the figure illustrates the introduction of a power adaptive mode to reduce the transmit spectrum, simultaneously reducing the interference on adjacent subscriber lines. DSM at level 1 can to a great extent be implemented on existing DSL service platforms without any requirements to hardware upgrades [18].

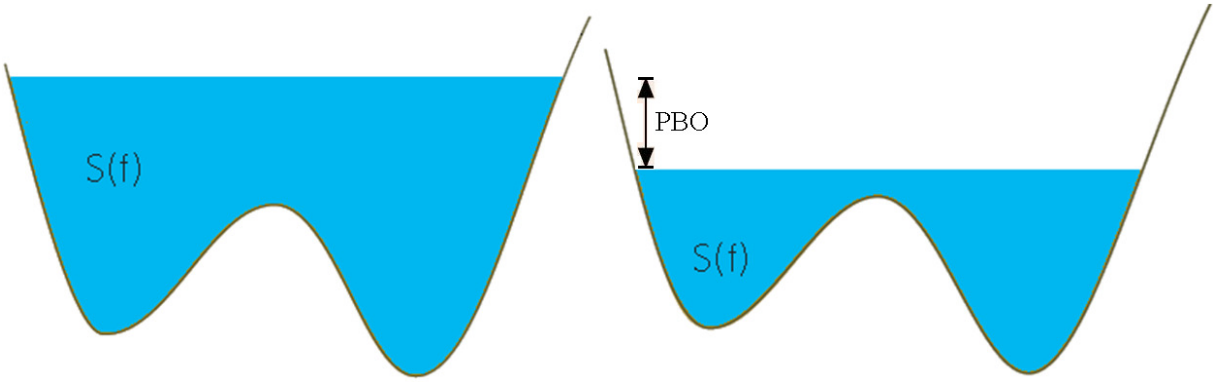

Figure 5: Hogging vs. Politeness

The left figure illustrates a system transmitting superfluous power "hogging" the resources while the right figure illustrates a system performing a polite use of the medium.

At DSM level 2 a centralized Spectrum Maintenance Center (SMC) performs coordination between the different subscribers in a binder. In contrast to DSM level 1, the subscriber lines' interfering crosstalk and cable lengths are collected by the SMC. This information is then used to adjust the different lines' transmitted PSD with a coordinated power allocation scheme to jointly optimize the transmitted spectrum [18]. Two similar algorithms for DSM level 2 is described in [19] and [20] denoted Optimal Spectrum Management (OSM) and Optimal Spectrum Balancing (OSB) respectively. DSM at level 3 exploits vectored DSL access multiplexing (DSLAM) for specification of the transmit PSD of each subscriber line. The vectors are decided based on the identification of the crosstalk's transfer functions where both amplitude and phase are important characteristics. The latest literature suggests bit rates approaching 0.5 Gbps on a single twisted pair for the highest degree of coordination at DSM

level 3 [19]. Research on bonding between different twisted pairs in a multiple input multiple output (MIMO) system implies even further capacity increase [21]. An overview of the DSM levels is given in table 2 with promising algorithms mentioned in parenthesis.

Table 2: Dynamic spectrum management levels

DSM level 0.	Static Spectrum Management
DSM level 1.	Distributed power control (IWF or ASB)
DSM level 2.	Centralized coordination in an SMC (OSB)
DSM level 3.	DSLAM vectoring and bonding with MIMO

2.4. Water-Filling

Water-filling is a well known algorithm to decide the power allocation and the information distribution of a communication system, with or without coordination [22]. As one of the most prosperous algorithms for DSM level 1, water-filling utilize fast bit loading techniques based on the channel signal-to-noise ratio, described as the signal-to-noise ratio (SNR) with unit signal power across the entire frequency band [23]. To optimize the resource allocation in a multiuser environment, functions for optimal bit rates are investigated. A cost function for optimal bit rates are presented by Bostoen et.al [12] and reproduced in the following formula:

$$\begin{aligned} \mathrm{J}\big(\mathrm{P_1(k)P_2(k)}\big) = &\sum_k log_2\left(1+\frac{h_{11}^2(k)P_1(k)}{\Gamma_1(h_{12}^2(k)P_2(k)+N_1(k))}\right) \\ &+\sum_k log_2\left(1+\frac{h_{22}^2(k)P_2(k)}{\Gamma_2\big(h_{21}^2(k)P_1(k)+N_2(k)\big)}\right) \\ &+\lambda_1\left(P_{1,con}-\sum_k P_1(k)\right) \\ &+\lambda_2\left(P_{2,con}-\sum_k P_2(k)\right) \end{aligned} \tag{8}$$

$P_n(k)$ refers to the power allocation for user n in carrier k, $h_{nn}^2(k)$ is the transfer function of the attenuation channel, Γ_n is the Shannon gap, $h_{nj}^2(k)$ is the transfer function of the crosstalk channel and $N_n(k)$ is the background noise power. λ_n is a constant in the Lagrange multipliers for solving the equation while taking into consideration the power restriction for both users given by the values of $P_{n,con}$. Deriving this through a dual decomposition [24] has been shown to give large performance gains. The need for an SMC to coordinate the lines will none the less increase the complexity of the modems and severely complicating the implementation of the algorithm [12]. However if the crosstalk power is assumed to be very

small compared to the background noise power, i.e.$\tilde{N}_1(k) \approx N_1(k)$, the cost functions can be simplified as in (9):

$$\begin{aligned} J\big(P_1(k)P_2(k)\big) = &\sum_k log_2\left(1+\frac{h_{11}^2(k)P_1(k)}{\Gamma_1+\tilde{N}_1(k)}\right) \\ &+\sum_k log_2\left(1+\frac{h_{22}^2(k)P_2(k)}{\Gamma_2+\tilde{N}_2(k)}\right) \\ &+\lambda_1\left(P_{1,con}-\sum_k P_1(k)\right) \\ &+\lambda_2\left(P_{2,con}-\sum_k P_2(k)\right) \end{aligned} \tag{9}$$

The optimum solution for user *n* is then found by taking the derivative of the cost function with respect to $P_n(k)$ and setting it equal to zero:

$$\frac{\partial J}{\partial P_n(k)} = \frac{1}{P_n(k)+\frac{\Gamma_n\tilde{N}_n(k)}{h_{nn}^2(k)}} - \lambda_n = 0 \tag{10}$$

Thus the water-filling equation is found by rewriting equation (10) as presented in (11):

$$P_n(k) = \frac{1}{\lambda_n} - \frac{\Gamma_n\tilde{N}_n(k)}{h_{nn}^2(k)} \tag{11}$$

By substituting the expression for the background noise power of $\tilde{N}_n(k)$ with an expression including interfering crosstalk, the formula for power allocation for iterative water-filling is obtained and presented for user 1 in a two-user environment:

$$P_1(k) = K_1 - \frac{\Gamma_1(h_{12}^2P_2(k)+N_1(k))}{h_{11}^2(k)} \tag{12}$$

K_1 is the upper limit of the transmit power in each carrier and consequently could be seen as the water level of the water-filling algorithm as illustrated in Figure 6. The fraction following the margin, Γ_1, is the inverse signal-to-noise ratio. The expression is sometimes denoted as the channel noise-to-signal (NSR) ratio or simply the noise-to-channel ratio (NCR), concisely characterizing the channel. In this thesis the Shannon gap is constant for all calculations and shall for convenience be included in the NCR, thus the previous expression simplifies to (13):

$$P_1(k) = K_1 - NCR_1(k) \tag{13}$$

$NCR_1(k)$ is consequently the noise-to-signal ratio of carrier k, including the Shannon gap. Figure 6 illustrates the water-filling of user 1 in a multiuser environment. The transmit spectrum is allocated to the different carriers in DMT transmission as if power was “poured” over the noise-to-channel ratio as water is poured into a bucket.

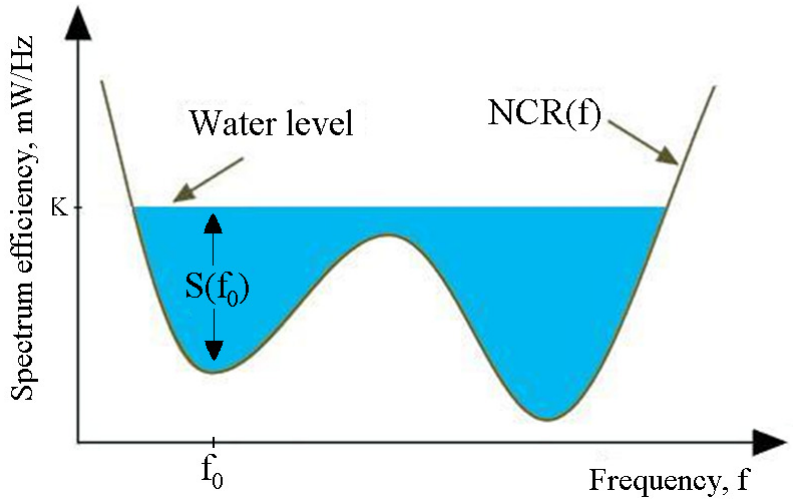

Figure 6: Water-filling

The figure presents water-filling power allocation filling up the transmit spectrum as pouring water into a bucket. The water-filling continues until a predefined water level is reached.

DSM at level 1 models the interference channel as a non-cooperative game and lets the power-allocation of each user be water-filled in an iterative manner denoted the iterative water-filling algorithm (IWF). This algorithm lets each subscriber adjust its own transmitted spectrum and thus avoids the need for centralized coordination. The objective of the algorithm is to reach a common optimality where each subscriber reaches their own bit rate maxima corresponding to the interfering noise, thus having no incentive to change its transmitted spectrum. In game theory this common optimality is denoted the Nash equilibrium and is described as a profile of strategies such that each player's strategy is an optimal response to the other players' strategies [26 p. 11]. In the two-user case; IWF starts by allocating an arbitrary power distribution to subscriber 1 and then lets each user update its transmitted power spectral density iteratively as in (13) regarding the interference from the other users as noise. The iterations end when the equilibrium is met. Abandoning the idea of spectral masks and allowing boosting for some frequencies will however, according to method A of the spectrum management standard [25], imply the possibility of a breach of the spectral compatibility with other services. Since iterative water-filling is operated in a fixed margin mode, in contrast to the regular margin adaptive mode, water-filling could also cause a considerable reduction to the noise margin. This suggests shorter lines could go out of sync when introducing new lines and the problem thus needs to be dealt with thoroughly [12].

2.5. System Variables

The system presented in this report were analyzed for Very High Bit Rate Digital Subscriber Lines (VDSL) as defined by band plan A, i.e. band plan 998, from the International Telecommunication Union's (ITU) recommendation G.993.1 [27]. This standard uses frequency-division duplexing (FDD) to separate between upstream- and downstream communication, and thus justify previous assumptions of zero NEXT. The frequency band utilized in this particular report was the lower band for upstream communication, denoted US1 in Figure 7. This band has a lower bound of; FL = 3.75 MHz and an upper bound of; FH = 5.2 MHz, resulting in a total bandwidth of; W = 1.45 MHz.

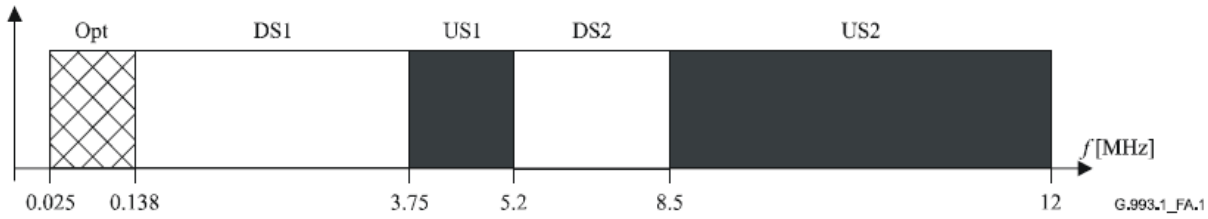

Figure 7: Frequency-Division Duplexing in VDSL [27]

The lower frequency band for upstream transmission denoted US1 is applied for all systems in this thesis.

The bandwidth is then split in 336 carriers to match the standard carrier bandwidth in discrete multi-tone modulation of; W_c = 4.3125 kHz. An initial fixed value for the transmit power spectral density (PSD) is given in (14):

$$S(f) = S_0 = -52\ dBm/Hz \tag{14}$$

This spectrum was allocated for all calculations at static spectrum management and will be referred to as the spectrum at nominal value or merely the fixed spectrum. Similar equation is given for the total noise spectrum different from self FEXT in (15), which remains unchanged throughout all calculations.

$$N(f) = N_0 = -140\ dBm/Hz \tag{15}$$

The Shannon gap was predefined at 5 dB which includes a safety margin of 1 dB:

$$\Gamma_n = 10^{0.5} = 3.16 \tag{16}$$

The logarithmic value for the crosstalk coupling coefficient relative to the proportionality constant denoted K_{FEXT} in (2) describing the crosstalk coupling at carrier frequency of 1 MHz and common cable length of 1 km is given in (17):

$$K_{FEXT} = 10^{-4.5}\ \frac{1}{MHz^2 \cdot km} \tag{17}$$

Hence the calculation of the far-end crosstalk power transfer function between subscriber i and subscriber j is presented in (18) relative to the multi-user expression in (2):

$$|H_{ij}(f)|^2 = K_{FEXT} \cdot F^2 \cdot L_{i,j} \cdot |H_{channel}(f)|^2 \quad (18)$$

F is thus the frequency in MHz while $L_{i,j}$ is the cable length in numbers of km where the disturbing and disturbed twisted pairs share the same binder. The channel transfer function $H_{channel}(f)$ is the attenuation of the interfering signal as it propagates from its transmitter to where it exits the common binder. In the case with two co-located receivers in the CO this attenuation is thus equal to direct channel of the disturber, i.e. $H_{channel}(f) = H_{jj}(f)$. The transfer functions of a two-user environment are illustrated in Figure 4 and given by equation (19) to (22):

$$|H_{11}(f)|^2 = L_1 \cdot \alpha \cdot \sqrt{f} \quad (19)$$

$$|H_{22}(f)|^2 = L_2 \cdot \alpha \cdot \sqrt{f} \quad (20)$$

$$|H_{21}(f)|^2 = K_{FEXT} \cdot F^2 \cdot L_{2,1} \cdot |H_{11}(f)|^2 \quad (21)$$

$$|H_{12}(f)|^2 = K_{FEXT} \cdot F^2 \cdot L_{1,2} \cdot |H_{22}(f)|^2 \quad (22)$$

L_1 and L_2 are here the lengths of the twisted pairs of user 1 and user 2 while α is the attenuation at 1 MHz predefined at; α = 22.5 dB/km/MHz. The indexes of the transfer functions denote the receiver and the transmitter of the channel respectively. Hence $|H_{11}(f)|^2$ and $|H_{22}(f)|^2$ are the transfer functions of the direct channel while $|H_{21}(f)|^2$ and $|H_{12}(f)|^2$ are the transfer functions of the crosstalk channels. $L_{2,1}$ and $L_{1,2}$ are obviously identical since they indicate the common binder length of L_1 and L_2. The crosstalk interference is finally attained by multiplication with the interfering signals' transmit power spectral densities; $S_1(f)$ and $S_2(f)$. Equation (23) and (24) present the crosstalk interference power spectral density in mW/Hz for user 1 and user 2 respectively in a two-user environment:

$$FE_1 = |H_{12}(f)|^2 \cdot S_2(f) \quad (23)$$

$$FE_2 = |H_{21}(f)|^2 \cdot S_1(f) \quad (24)$$

The crosstalk interference is added to the background noise given by $N(f)$ and compared to the transmit spectrum in $S(f)$ to calculate the signal-to-noise ratio as in (4) and (5). Thus an expression for the bit rate can be presented as the summation of the bit rate in each carrier:

$$R = \frac{1}{T} \sum_{k=1}^{K} log_2\left(1 + \frac{SNR(k)}{\Gamma}\right) \quad (25)$$

T is the period of the carrier bandwidth while K is the number of carriers in the DMT modulation previously set to 336. $SNR(k)$ is the signal-to-noise ratio of carrier k and Γ is the Shannon gap as described in Chapter 2.2. Substituting the SNR for the transfer functions,

noise and interference, as shown in Chapter 2.4, provides the full expression for the total transmission rate as used in the calculations, here presented for subscriber 1 in the two-user environment:

$$R_1 = \frac{1}{T}\sum_{k=1}^{K} log_2\left(1 + \frac{|H_{11}(f)|^2 S_1(f)}{\Gamma_1(|H_{21}(f)|^2 S_2(f) + N_1(f))}\right) \qquad (26)$$

A limitation to the bandwidth efficiency, i.e. a bandwidth efficiency maximum (BWEM), is also set at; BWEM = 15 b/s/Hz. This is due to difficulties introduced for systems with higher bandwidth efficiencies. The bandwidth efficiency maximum introduces a constraint to the maximum bit rate as presented in equation (27):

$$R_{max} = BWEM \cdot W \qquad (27)$$

W is as mentioned the bandwidth of US1 in Figure 7. Although VDSL systems introduce higher bandwidth efficiencies than ADSL, which typically works on approximately 6 b/s/Hz [28], the BWEM is seldom the constraint in a communication system.

2.6. Procedure

The implemented system consists of a 10-pair binder, initially analyzed with a fixed transmit spectrum in two active pairs of different cable length in static spectrum management. The other pairs in the binder are thus assumed to be inactive. A fixed power back-off (PBO) was then applied to the shortest line to reduce interfering crosstalk on the adjacent line. The PBO introduces a direct reduction to the transmit spectrum given by $S(f)$ in (14), thus a PBO of 3 dB would imply the transmit PSD is reduced to half, calculated by inserting the values into (28):

$$S(f) = S_0 - PBO \qquad (28)$$

Secondly the iterative bit loading algorithm is presented, introducing a dynamic transmit spectrum with unequal power allocation for the different carriers. Thirdly, the most prosperous algorithm for DSM at level 1 and the main algorithm of this report; water-filling, is described and implemented in the two-user environment. The iterative water-filling, which is based on the water-filling algorithm, was implemented next and is also imperative for the consecutive results in this report. Some calculations were performed with increased differences in the cable length of the two twisted pairs in the system for better presentation of the water-filling basics. Then a PSD constraint was applied to the water-filling algorithm to avoid peaks in the transmitted spectrum and consequently high values of peak-to-average ratio (PAR). The PSD was constrained to a maximum of twice the nominal value:

$$S(f) \leq S_0 + 3\ dB \quad (29)$$

A new algorithm for dynamic spectrum management was presented with the implementation of top-filling with maximum bit efficiency allocated iteratively to the carriers. The algorithm starts at the highest frequencies and terminates when a rate constraint is reached. The final three subchapters include implementation of multi-user environments where several of the mentioned algorithms were applied. These subchapters also introduced differentiation in the crosstalk coupling based on empirical research. Both rate adaptive mode and power adaptive mode were implemented illustrated with the longer line attaining a maximum bit rate while the shorter lines applied power back-off if a rate constraint was reached. All algorithms have been implemented in MATLAB® and could be accessed through NTNU's digital archives for submitted master thesis (DAIM).

3. RESULTS

First, there will be given a presentation of the static spectrum management approach with a fixed spectrum level for all the carriers before different DSM algorithms are presented in the succeeding parts. The discussion of each algorithm presented in the following sections in this chapter is exclusively presented in Chapter 4.

3.1. Fixed Spectrum

The initial implemented system for calculations included two active pairs denoted L_1 and L_2 with lengths of 800 meters and 500 meters respectively. The lines are thought of as autonomous lines in upstream DSL communication with transmitters in the remote end and receivers in the central office, as illustrated in Figure 8:

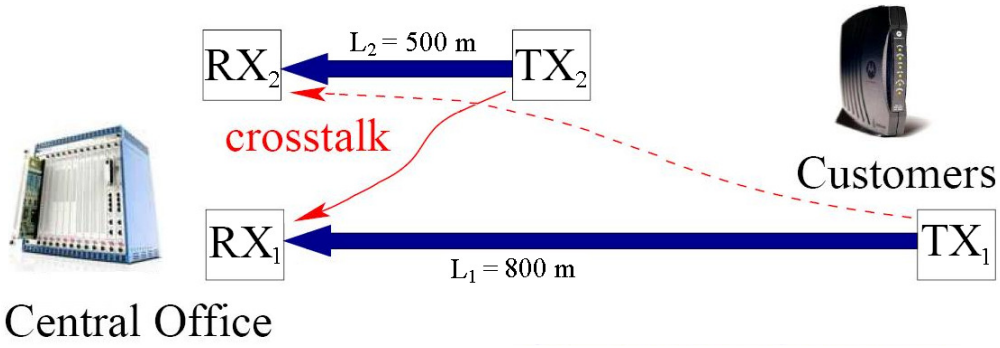

Figure 8: Two active subscribers

The figure presents two twisted pairs of lengths 800 and 500 meters.

3.1.1. Full power on two active lines

A fixed spectrum at nominal value was transmitted in both subscriber lines, i.e. $S(f) = S_0$ as in (14). The transmitted power was thus equal for both lines and given by the following expression:

$$P = S_0 \cdot W = -52 \frac{dBm}{Hz} \cdot 1.45\ MHz = 9.15\ mW \qquad (30)$$

This value was set as the maximum permitted transmit power and used as a constraint for the subsequent algorithms. The common binder length was set and calculations of the interfering crosstalk- and attenuation channels were performed as in (19) to (22) with successive computation of the system capacities as in (25). The resulting bit rate for the shortest line was calculated at; R_2 = 20.30 Mbps, while the longer line achieved a bit rate of; R_1 = 6.87 Mbps. The references to the bit rates R_1 and R_2 should not be confused with the notation of RX_1 and RX_2 for the receivers in Figure 8.

3.1.2. Introducing Power Back-Off

Last section's calculations revealed the shortest line achieved a great bit rate compared to the longer line when both were transmitting at full power. Subscribers with transmitters as close to the CO as T_2 in Figure 8 often introduce critical interference to subscribers farther away, as presented in the theory of the Near-Far problem in Chapter 2.1.3. Thus, a PBO to the transmitted power in L_2 would imply a more balanced distribution of the capacity between the subscribers. By the method of trial and error a PBO of 11.1 dB was found when approximating a wanted bit rate for the shortest line of; $R_1 = 15$ Mbps. The transmitted spectrum of the shortest subscriber line can be calculated by inserting the nominal value for the transmitted spectrum and the mentioned PBO into (28) as in (31):

$$S_2(f) = -52\ \frac{dBm}{Hz} - 11.1\ dB = -63.1\ \frac{dBm}{Hz} \qquad (31)$$

The altered value for the interfering transmit PSD is inserted in (26) resulting in a bit rate for the longest line now increased to; $R_1 = 12.23$ Mbps.

3.1.3. Presenting the Rate Region

By systematically increasing the power back-off in of the shortest line as in (31) with successive calculation of the bit rates for both lines as in (26), the resulting bit rate pairs represent a rate region for the two twisted pairs. A set of 17 different PBOs was chosen carefully to present a continuous graph for the rate region as presented in Figure 9. Each calculated bit rate pair is presented by a cross in the figure. The figure clearly illustrates a reduction in the bit rate of the shortest pair as the PBO increases. The longest pair experiences in contradiction an increase to its bit rate, proportional to the PBO in the disturber.

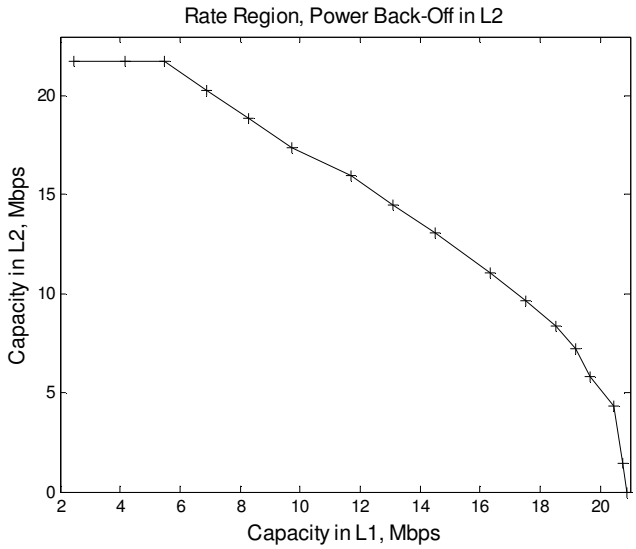

Figure 9: Rate Region with Static Spectrum Management

The figure presents the rate region with an increasing flat power back-off to the shortest line L_2.

For better illustration also negative PBOs were permitted, allowing a boost to the transmitted spectrum for the shortest line. Hence, the bit rate of L_2 reached the capacity limited by the product of the bandwidth and the bandwidth efficiency maximum given by equation (27), as seen by the bit rate pairs to the far left in Figure 9. The PBOs given in Table 3 below were applied to the shortest pair when calculating the capacities of the twisted pair. The PBO of -10 dB thus corresponds to the leftmost cross in the rate region while the bottom right cross corresponds to a PBO of 50 dB.

Table 3: Fixed PBO in the shortest line

Boosting:	-10	-6	-3										
PBO:	0	3	6	10	13	16	20	23	26	28	30	35	40	50

3.2. Single-bit Bit Loading

As presented in Chapter 2.2, DSL exploits the characteristics of DMT to allow separate bit loading for each carrier in multi carrier modulation. The total achieved bit rate is given by (5) and repeated for convenience here:

$$b_1(k) = log_2\left(1 + \frac{|H_{11}(k)|^2 P_1(k)}{\Gamma_1(|H_{12}(k)|^2 P_2(k) + N_1(k))}\right) \qquad (32)$$

As stated in Chapter 2.2; b_k^1 is the bit loading in the k'th carrier in for subscriber line 1, $h_{11}^2(k)$ is its channel attenuation, $P_1(k)$ and $P_2(k)$ are the transmitted powers in carrier k for subscriber 1 and 2 respectively, Γ_1 is the Shannon gap and $N_1(k)$ is the additiv noise power. By rewriting (32), an expression for the transmit power required to transmit i bits in the carrier can be found as in (33).

$$P_1^i(k) = (2^i - 1)\cdot \frac{\Gamma_1(|H_{12}(k)|^2 P_2(k) + N_1(k))}{|H_{11}(k)|^2} \qquad (33)$$

By substituting the fraction in (33) with the noise-to-channel ratio as in (13) a simplified equation is given in (34):

$$P_1^i(k) = (2^i - 1)\cdot NCR_1(k) \qquad (34)$$

Consequently, an expression for the additional power to transmit another bit in carrier k when i bits already are loaded to the carrier is given by the difference of the power allocation of $P_1^{i+1}(k)$ and $P_1^i(k)$:

$$\Delta P_1^i(k) = P_1^{i+1}(k) - P_1^i(k) = 2^i \cdot NCR_1(k) \qquad (35)$$

A logarithmic, recursive expression is found by comparing the additional power to load the $(i+1)$'th bit and the i'th bit to a carrier:

$$\Delta P_1^{i+1}(k)_{dB} = \Delta P_1^{i}(k)_{dB} + 3dB \qquad (36)$$

Hence, the additional power required to load another bit to the carrier is twice the additional power required to load the previous bit. The "single-bit" bit loading presented in this chapter alternately add one bit to the carrier where the least additional power is required. Simultaneously, this carrier's required power to load another bit is increased as defined in (36) and the algorithm continues searching for the carrier where the least additional power is required. The algorithm initially terminated when the carrier with the highest power spectral density reached the nominal value given by S_0 in (14) and resulted in a bit rate of; R_1 = 6.86 Mbps. However, the left illustration of Figure 10 evidently shows the transmit PSD on an average is significantly lower than the fixed spectrum at nominal value illustrated by the dashed line in the figure. The total transmit power is reduced to 6.32 mW.out of the permitted 9.15 mW calculated in (30). Still the system maintains the same bit rate as found in the previous section's fixed spectrum analysis. With the abillites of a dynamic spectrum this superfluous power can instead be shifted to carriers where an increse in the bit loading is possible. Hence, the algorithm's terminating constraint was altered to the total transmitted power and the algorithm was implemented as described by Algorithm 1. The single-bit bit loading approach now transmits an average PSD equal to the fixed spectrum approach resulting in a bit rate of; R_1 = 7.61 Mbps. The right illustration of Figure 10 presents the transmitted spectrum with the total power at fixed spectrum as the terminating constraint. When introducing a PBO of 11.1 dB to the interfering subscriber line's transmitted PSD, as in Chapter 3.1.2, the resulting bit rate was increased to; R_1 = 12.87 Mbps.

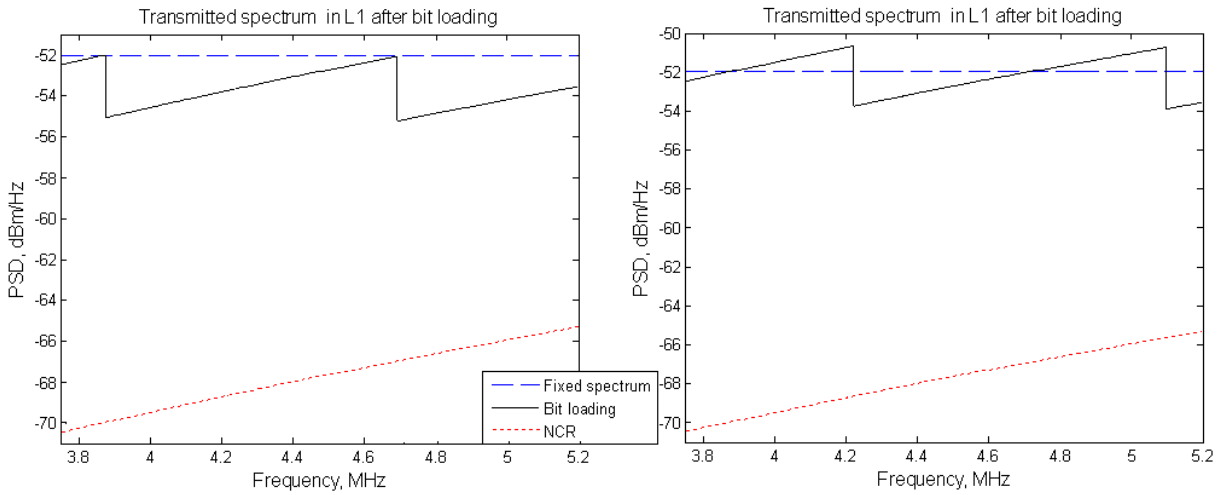

Figure 10: Bit loading

The left figure presents the transmitted PSD terminated by a PSD constraint, while the right figure presents bit loading with a power constraint equal the power at fixed spectrum.

The bit loading algorithm is summarized in the following:

Algorithm 1: Let ***k*** be the carrier index of the carrier which requires the least additional power; ΔP_k, to allocate another bit to its bitloading; ***b***. Let ***NCR*** be the input noise-to-channel ratio and W_c; the carrier bandwidth. Let *P* be the total power, P_{max}; the available power and P_k; the output power allocation.

initialize
  for all carriers k Є K **set** ($\Delta P_k = NCR_k$; $b_k = 0$; $P_k = 0$)
repeat
  set $b_k = b_k + 1$
  set $P_k = P_k + \Delta P_k$
  set $\Delta P_k = 2 \cdot \Delta P_k$
  set $P = \sum_{j=k}^{K} P_k$
  set $k = \arg\min\{\Delta P_k\}$
until $P \geq P_{max}$

3.3. Water-Filling

The bit loading approach presented in the previous section works well if convergence speed is not an important feature. The water-filling algorithm, as described in Chapter 2.4, was thus introduced in the calculations for a faster power allocation. The calculations were performed on the same systems as in the previous sections with distances of 800 meters and 500 meters for L_1 and L_2 respectively. As in the case of static spectrum management in Chapter 3.1.2, a PBO of 11.1 dB was applied to L_2 to balance the bit rates better. The spectrum of the shortest line was thus set to the same fixed value as in (31), i.e. $S_2(f) = S_0$. The water-filling algorithm was then performed to decide the power allocation in L_1. Figure 11 illustrates the transmit power spectral density of L_1 after water-filling is performed:

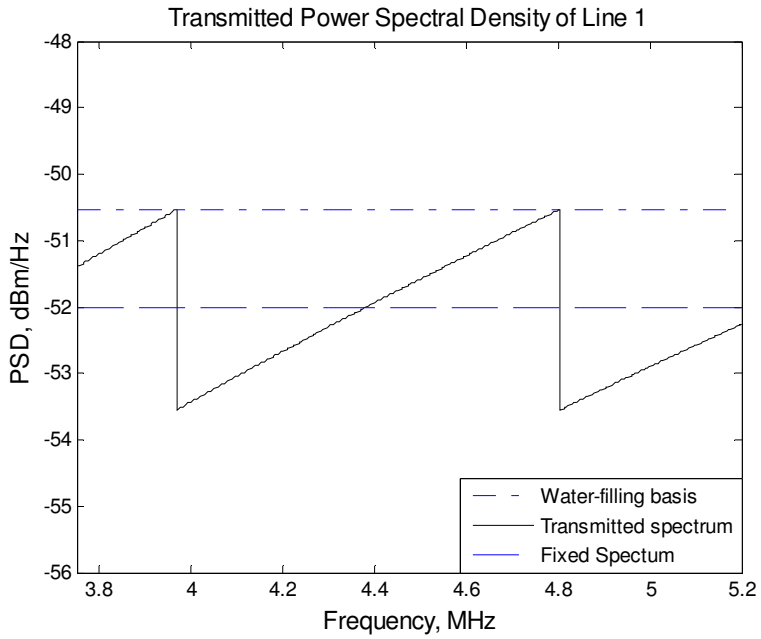

Figure 11: Water-Filling

The figure illustrates the transmit spectrum of the longest line after water-filling.

The dash-dotted line denoted *water-filling basis* corresponds to spectrum of the transmit power allocation in (13). Obviously this spectrum exceeds the permitted average spectrum given by S_0 in (14) illustrated in the figure by the dashed line denoted *fixed spectrum*. In these calculations however; the water-filling line represents only the basis for the bit allocation which successively decides the transmit spectrum as illustrated by the black, drawn graph. The big "steps" in the transmit spectrum thus correspond to the reduction of a bit in the bit loading when the NCR is continuously increasing. Consequently, power allocation in the carriers above ~ 4 MHz permits a signal constellation of 1 bit less than the lower carriers. Similarly, the power allocation at carriers higher than ~ 4.8 MHz implies a signal constellation degradation of 2 bits. The water-filling line should neither be confused with the water level of the algorithm which is the summation of the water-filled spectrum and the noise-to-channel ratio, as presented in (13). Hence, the average transmit spectrum equals the nominal value, i.e. $mean(S_1(f)) = S_0$. The algorithm's resulting bit rate is; R_1 = 12.87 Mbps. To illustrate the water-filling better a fictitious penalty to the SNR was applied as if the signal picked up an extra attenuation or experienced additional noise. Water-filling of L_1 with a SNR penalty of 13 dB and an interfering fixed spectrum at nominal value is illustrated in Figure 12:

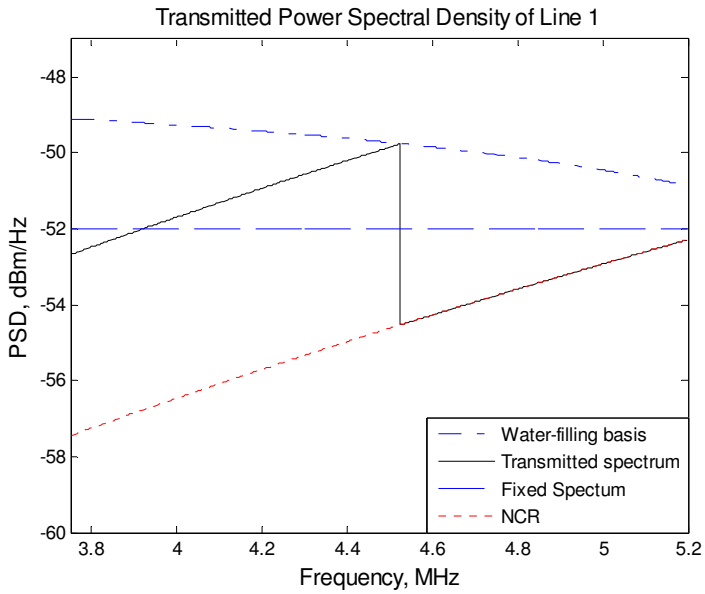

Figure 12: Water-Filling with severe penalty to the SNR

The figure illustrates water-filling when a powerful penalty is applied to the SNR

The resulting bit rate achieved by water-filling was calculated at; R_1 = 2.22 Mbps. When a fixed spectrum at nominal value was applied to the same system, calculations resulted in a bit rate of; R_{ssm} = 1.62 Mbps.

3.4.Iterative Water-filling

The water-filling algorithm presented in the previous section can be autonomously executed on each twisted pair in an iterative approach denoted iterative water-filling described in the last section of Chapter 2.4. The objective of the algorithm presented in this section was to maximize the bit rate of an interference impaired DSL subscriber while maintaining an acceptable bit rate in any interfering line. Consequently, an upper limit for the bit rate of the shortest line in the previously presented system was included in the algorithm. The constraint was set equal the bit rate at fixed spectrum with flat power back-off as given in Chapter 3.1.2. Thus, a bit rate of 15 Mbps was set as a terminating constraint to the water-filling algorithm, with successive calculations of the bit rate as in (26). Figure 13 presents the transmit power spectral density in L_2 compared to the PSD of the fixed spectrum where no rate constraint is applied.

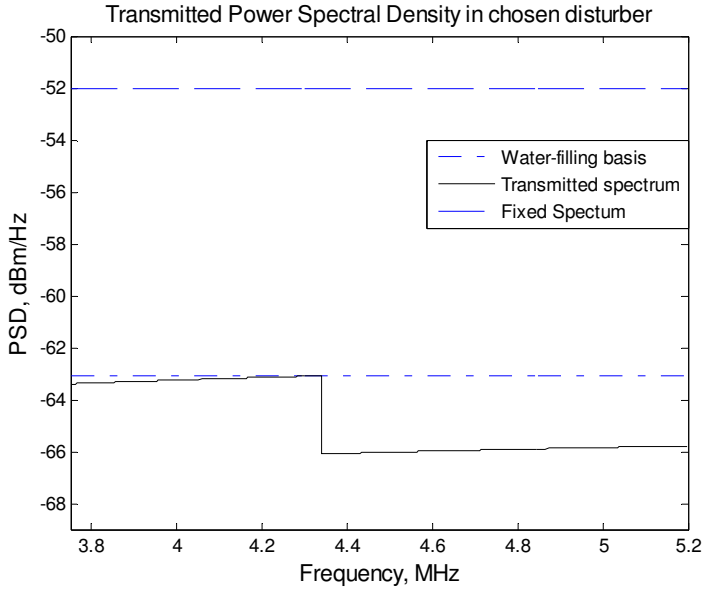

Figure 13: Water-filling of interferer constrained by bit rate

The figure illustrates the transmitted spectrum in the shortest line with a rate constraint of 15 Mbps.

The dash-dotted line illustrating the water-filling basis is almost identical to the transmitted spectrum when a flat PBO of 11.1 dB was introduced in the previous sections. The actual transmitted spectrum, illustrated by the drawn graph, implies a significant reduction in the crosstalk interference disturbing the longer line. Calculations return a total transmitted power of; $P_2 = 0.5$ mW and an average reduction to the PSD of 1.7 dB compared to the transmit spectrum with flat PBO. The water-filling algorithm is then performed on the longest line, illustrated by the transmit spectrum in Figure 14.

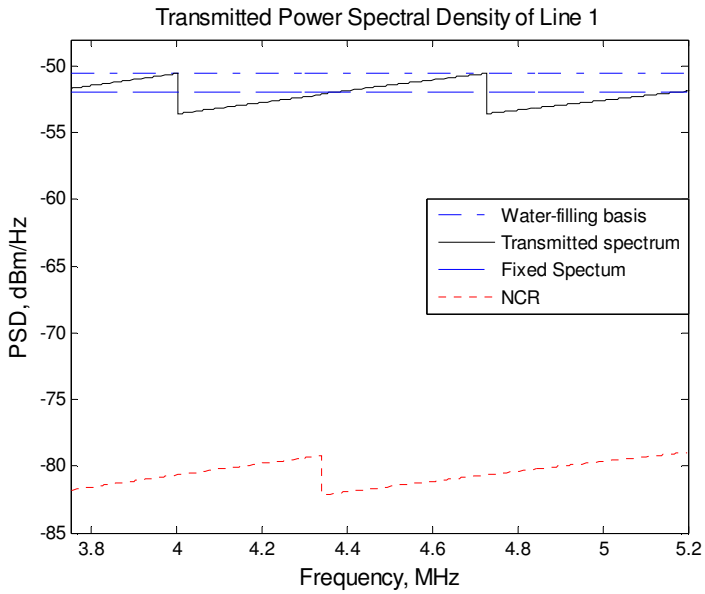

Figure 14: Water-Filling with water-filled interferer

The disturber itself has now been water-filled and contributes with less interference.

The resulting bit rate is now; R_1 = 13.69 Mbps. The iterative water-filling algorithm calculates the new interference from L_1 and runs the water-filling algorithm for the shortest line a second time, resulting in new adjustments to the transmitted PSD and consequently also on the interfering crosstalk. Water-filling is for the second time applied to L_1 with new calculations of the interference and so forth until the transmit PSDs reach convergence, as described by the Nash equilibrium in Chapter 2.4. After five iterations of water-filling for each line a bit rate of; R_1 = 13.79 Mbps was achieved for L_1, still maintaining the same bit rate of; R_2 = 15 Mbps in L_2. A rate region of the bit rate pairs in the two subscriber lines is presented in Figure 15.

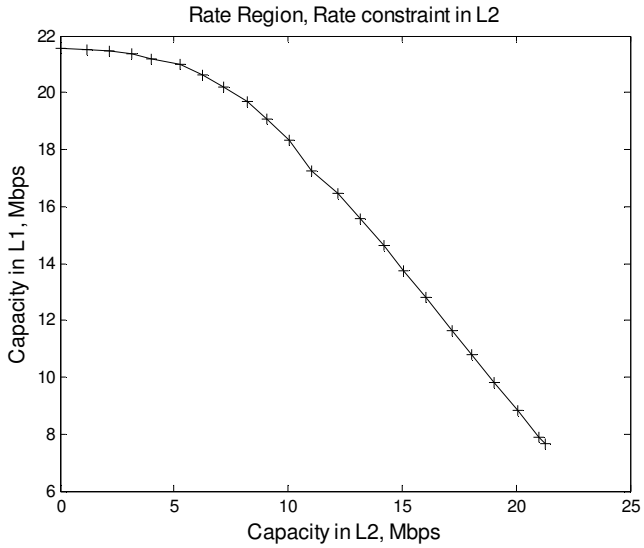

Figure 15: Rate Region of the iterative water-filling algorithm

The bit rate pairs illustrate a rate region for two twisted pairs of lengths 500 and 800 meters as.

The rate region is obtained by increasing the rate constraint of the shortest line, similar to the increase in the applied PBO when presenting the rate region for SSM in Chapter 3.1.3. Consequently, every cross in the rate region corresponds to a preset constraint to the capacity of the shortest line. The iterative water-filling algorithm is summarized as follows:

Algorithm 2: Let i be the i'th user in an M-user environment. Let $\acute{N}_i(f)$ be the total noise spectrum with crosstalk channel; $H_{ij}(f)$, interfering spectrum; $S_j(f)$ and interfering noise different from fext; $N_i(f)$. Let $S_i(f)$ be the output transmit spectrum with water level K_i, Shannon gap Γ and attenuation transfer function $H_{ii}(f)$. Let P_i be the transmit power, FL and FH be the lower and upper bound of the bandwidth respectively, P_{con} be the power constraint, δ be the power accuracy and ε be the water level accuracy. Let R_i be the transmit bit rate and $R_{i,req}$ the required bit rate.

repeat
 for all users $i \in M$ **do**
  repeat
   set $\acute{N}_i(f) = \sum_{j=1,j\neq i}^{M}(|H_{ij}(f)|^2 S_j(f) + N_i(f))$
   set $S_i(f) = K_i - \Gamma \cdot \acute{N}_i(f)/|H_{ii}(f)|^2$
   set $P_i = \int_{FL}^{FH} S_i(f)\ df$
   if $P_i < P_{con} - \delta$, **set** $K_i = K_i + \varepsilon$
   if $P_i > P_{con} + \delta$, **set** $K_i = K_i - \varepsilon$
  until $(R_i \geq R_{i,req}$ **given** $P_i < P_{con} + \delta)$ **or** $|P_i - P_{con}| < \delta$
 end for
until all users' PSD converge

3.5. Great Differences in Cable Length

Water-filling can be better illustrated by reducing the length of the shortest line, similar to the case of a fictitious penalty in the signal-to-noise ratio in Chapter 3.3. The length of the disturbing line, L_2, is thus shortened to 300 meters, illustrated for convenience in Figure 16. The new value for common binder length is set with successive calculations of the attenuation as in (19) and (20) and the crosstalk coupling as in (21) and (22). Subsequent water-filling is performed in L_1, now only constrained by the total permitted power given in (30), resulting in a transmit power spectral density as illustrated in Figure 17.

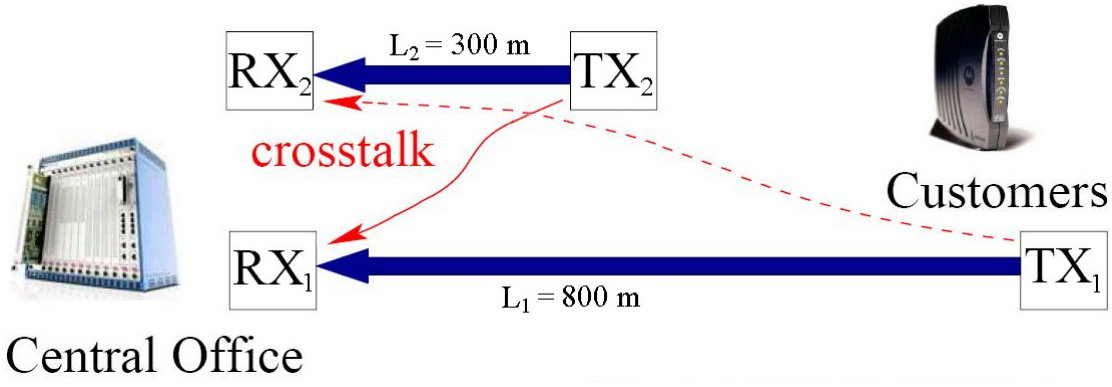

Figure 16: Increased differences in cable length

Water-filling is more visible at increased interference, presented here by a 300 meter long disturber.

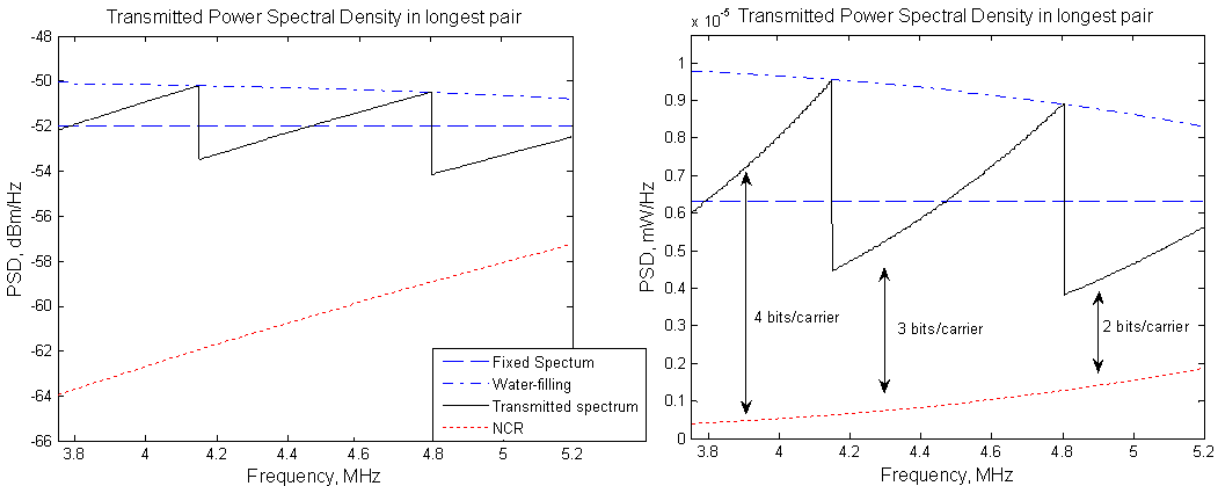

Figure 17: PSD with great differences in cable length

The figure to the left illustrates the spectrum with a logarithmic scale. The water-filling algorithm is however even more visible at a normal scale, presented in the right figure.

In addition to a logarithmic presentation in the left part of Figure 17, the figure includes an illustration of the spectrum in mW/Hz as the water-filling basics are even more perceptible in this domain. The figure illustrates L_1 dominated by a powerful disturber and the resulting bit rate is; $R_1 = 4.35$ Mbps. The capacities in L_1 with the same twisted pair lengths achieved by static spectrum management was; $R_{ssm} = 3.66$ Mbps. Additional calculations were performed with the cable length of the shortest line reduced to 100 meters resulting in bit rates of; $R_1 = 2.59$ Mbps and $R_{ssm} = 1.93$ Mbps.

3.6. PSD Constraint

Transmitting very high power in some carriers causes a greater peak-to-average ratio (PAR) and can lead to low power efficiency and possible nonlinear distortion [29]. A constraint to the highest permitted PSD for a carrier was thus applied to the water-filling algorithm. The constraint was predefined to 3 dB above the nominal spectrum as described in (29). The initial straight forward approach was to let the PSD constraint terminate the program immediately upon verification. Hence, the power allocation would terminate when the constraint was reached, leading to a transmitted power beneath the permitted level. The initial lengths of the twisted pairs were set to 900 meters and 100 meters and calculations were performed to obtain the system parameters as in (19) to (22) prior to the execution of the water-filling algorithm in the longest pair, L_1. The left part of Figure 18 illustrates the power spectral density after L_1 is water-filled with the immediate termination of the algorithm when the PSD constraint is reached. The algorithm was then evolved to shift its spectrum from carriers where the constraint is exceeded to carriers with less power spectral density. The result is presented in

the right part of Figure 18. This returned an increase of the bit rate by 22.5 percent compared to the straight forward approach.

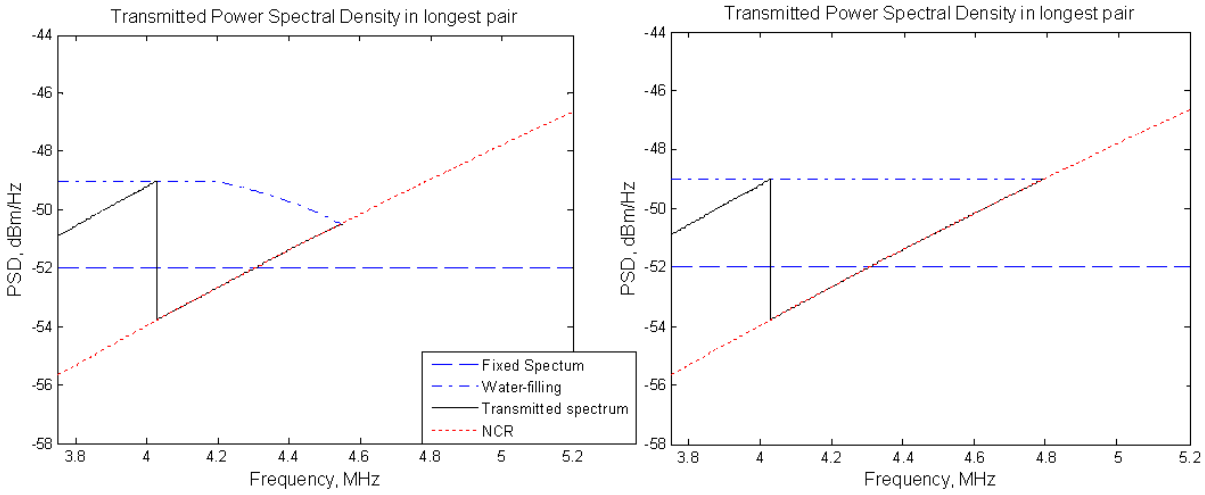

Figure 18: Transmitted spectrum with a PSD constraint

The figure to the left presents the straight forward approach of terminating the algorithm when the PSD constraint is reached. The figure to the right illustrates the algorithm which shifts the transmitted spectrum to other frequency bands and only terminates when the permitted power is reached.

The cable length of L_2 was then increased to 200 meters and calculations of both with- and without a PSD constraint was completed. The returned bit rates are 1.72 Mbps and 1.73 Mbps respectively when both transmit the permitted power. The transmitted spectrums are shown in Figure 19.

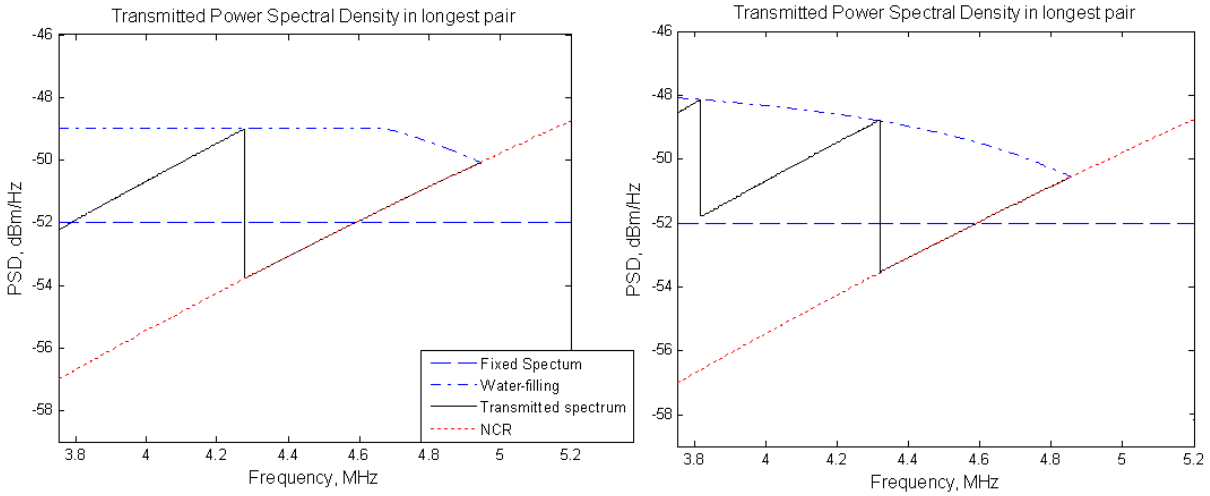

Figure 19: Transmitted spectrum with a PSD constraint II

The figure to the left presents the water-filling of a system with a constraint to the PSD. The algorithm to the right does not apply the constraint with resulting higher peak to average ratio.

3.7. Top-Filling

Another algorithm for dynamic spectrum management was here designed and implemented in particular to study the effect of the ability to "turn of" different tones, as experience with the

water-filling algorithm when the NCR exceeds the water-level. The objective of the algorithm was to allocate a maximum number of bits, limited by the BWEM, to the upper frequency bands of an interfering line in a two-user environment. The top-filling algorithm starts the power allocation at the carrier with the highest frequency, hence the name *top*-filling, and terminates when a predefined bit rate constraint is reached or if the permitted power is exceeded. Every carrier at the lower frequency bands are thus shut off, eliminating all crosstalk interfering on other twisted pairs transmitting in these bands. To avoid extreme levels in the transmit PSD when transmitting in noisy environments; the mentioned PSD constraint was also applied to the top-filling algorithm to terminate the bit loading prior to achieving the BWEM in carriers with significant NCR. Excluding this constraint could cause the entire available power being allocated to interference dominated carriers, resulting in the total power constraint being met prior to achieving the required bit rate. An elucidative figure is given in Figure 20 illustrating a maximum power allocation to the carriers above ~ 4.2 MHz resulting in a crosstalk free frequency band below ~ 4.2 MHz.

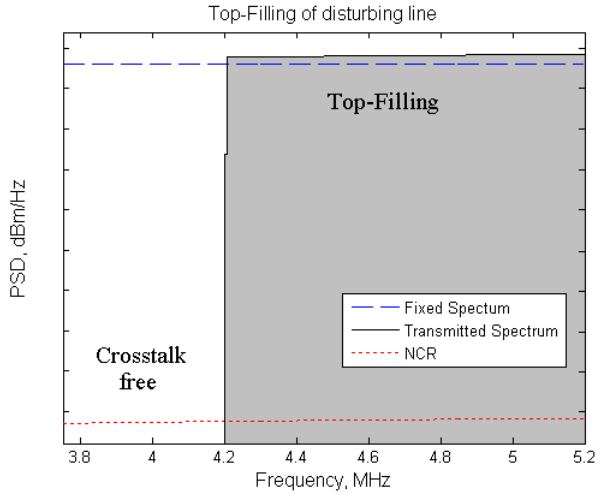

Figure 20: Top-Filling

The algorithm allocates power to the highest frequency tones and continues till a rate constraint is reached.

Top-filling with a bit rate constraint of 15 Mbps was applied to L_2 with subsequent water-filling perform in L_1, thus maximizing the bit efficiency in the lower frequency bands where no crosstalk from L_2 was present. Figure 21 illustrates the water-filled spectrum in L_1 once top-filling is applied to L_2. The NCR reveals severe crosstalk in the frequency band above ~ 4.2 MHz, while the frequency band below ~ 4.2 MHz is merely affected by attenuation and white noise.

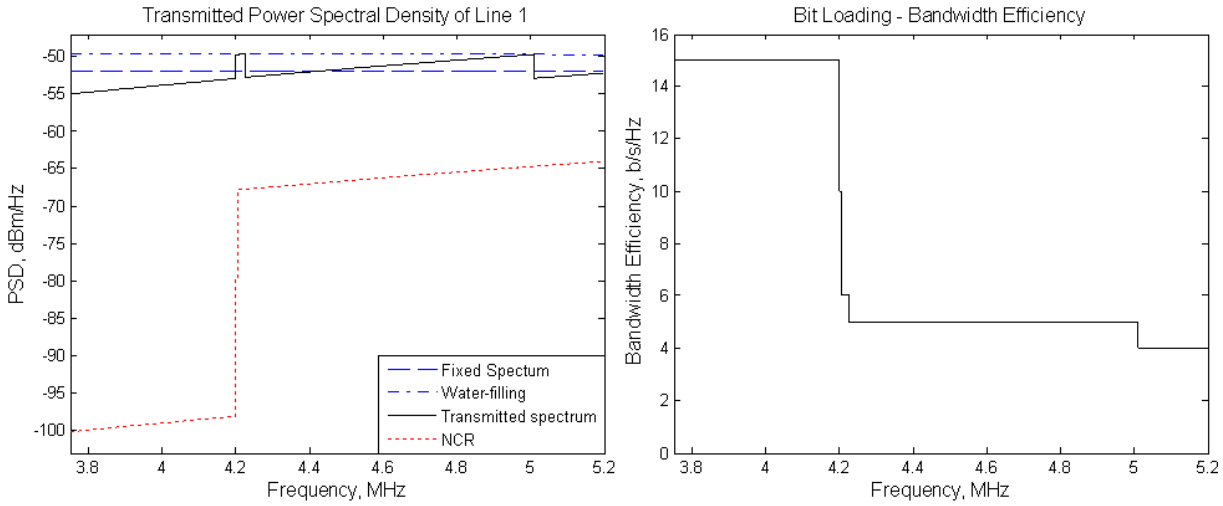

Figure 21: PSD and bandwidth efficiency with top-filling

The figure to the left illustrates the transmitted spectrum with severe interference in the higher bands. The figure to the right presents the corresponding bandwidth efficiency.

The bandwidth efficiency maximum at 15 b/s/Hz limits the bandwidth efficiency in the lower frequency bands and a relatively low PSD is allocated, as illustrated by the drawn, black line at frequencies lower than ~ 4.2MHz. As a consequence most of the power is allocated to the interference dominated bands. The bandwidth efficiency in Figure 21 illustrates that nearly 60 percent of the bits are transferred in the tones lower than ~ 4.2 MHz while calculations reveal that less than 20 percent of the total power is allocated in these bands. The bit rate achieved for L_1 when the interfering line executes top-filling was; R_1 = 11.59 Mbps. A rate region with alternately top-filling in L_2 and water-filling in L_1 was performed by increasing the wanted bit rate in L_2 and is illustrated in Figure 22:

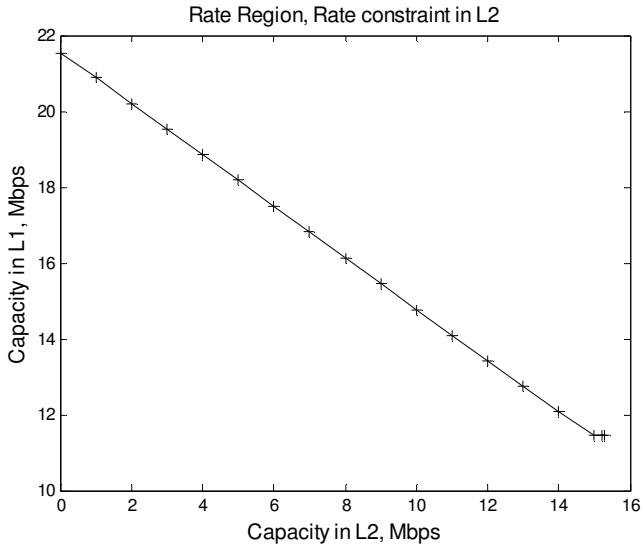

Figure 22: Rate region at top-filling

The rate region becomes a near linear graph since the top-filling of an interfering line with an increase to the required rate merely narrows down the usable frequency band for the interfered line.

The top-filling algorithm is summarized as follows:

Algorithm 3: Let $\boldsymbol{K}$ be the number of carriers, $\boldsymbol{P_k}$ be the power allocation and $\boldsymbol{P}$ be the total transmitted power. Let $\boldsymbol{\Delta P_k}$, be the additional power to allocate another bit to the carriers bitloading; $\boldsymbol{b_k}$. Let $\boldsymbol{BWEM}$ be the bandwidth efficiency maximum, $\boldsymbol{P_{k,con}}$ be the carrier power constraint, $\boldsymbol{P_{max}}$ be the available power, $\boldsymbol{R_{req}}$ be the required bit rate, $\boldsymbol{NCR_k}$ be the input noise-to-channel ratio and $\boldsymbol{R}$ be the output bit rate.

initialize
  for all carriers $k \in K$ **set** ($\Delta P_k = NCR_k$; $b_k = 0$; $P_k = 0$)
for all carriers $k \in K$ **do**
  repeat
    set $b_{K-k+1} = b_{K-k+1} + 1$
    set $P_{k-k+1} = P_{K-k+1} + \Delta P_{K-k+1}$
    set $\Delta P_{k-k+1} = 2 \cdot \Delta P_{k-k+1}$
    set $P = \sum_{j=k}^{K} P_k$
    set $R = \sum_{j=k}^{K} b_k$
until $b_{K-k+1} = BWEM$ **or** $P_{K-k+1} > P_{k,con}$ **or** $P > P_{max}$ **or** $R > R_{req}$
end for

3.8. Three Active Pairs

In the case of more than two active pairs, the algorithms for dynamic spectrum management are required to calculate the sum of the interferences from all the other active pairs in the binder. The total noise power in a three-user environment is thus the following summation, here presented for user 1:

$$\acute{N}_1 = WN + FE_2 + FE_3 \qquad (37)$$

WN is the additive white Gaussian noise power, identical in the expression for all three lines, while FE_2 and FE_3 are the interfering crosstalk from line 2 and line 3 respectively relative to (23) and (24). Initially the crosstalk coupling coefficients were set equal to the nominal coefficient given by K_{FEXT} in (17) and were thus equal for the coupling between all three lines. For convenience an illustration of the system is presented in Figure 23.

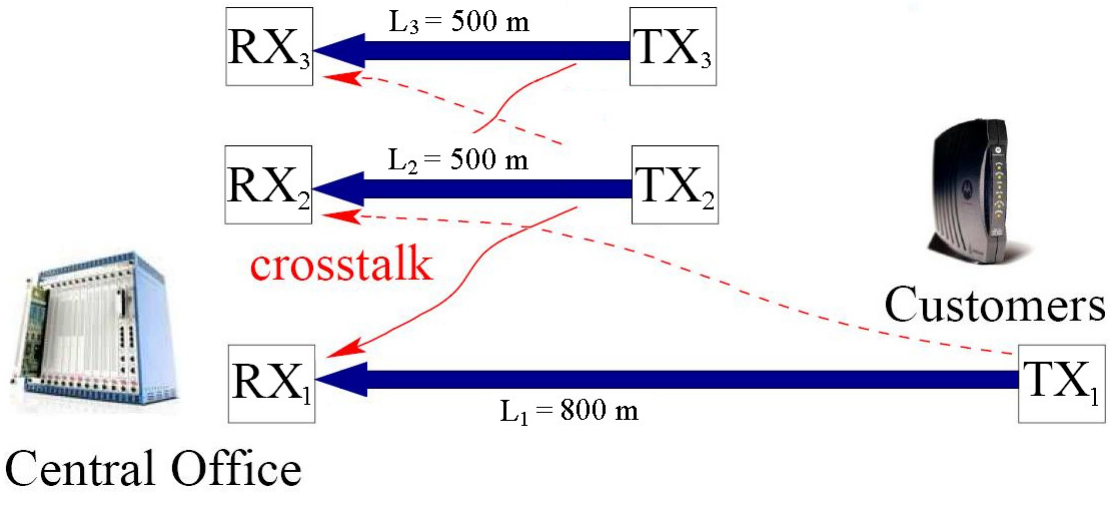

Figure 23: Three active subscriber lines

3.8.1. Fixed Spectrum

Similar calculations were performed in the three-user environment as was performed in the two-user environment in Chapter 3.1.1. The resulting capacities were; R_1 = 5.48 Mbps, R_2 = 13.63 Mbps and R_3 = 13.63 Mbps as presented in Table 4.

3.8.2. Water-Filling

The water-filling algorithm was executed for the longest line in the same manner as in the two-user case, regarding the interference from both L_2 and L_3 as additive noise. The transmitted power spectral density is illustrated in Figure 24, resulting in a bit rate of; R_1 = 6.22 Mbps.

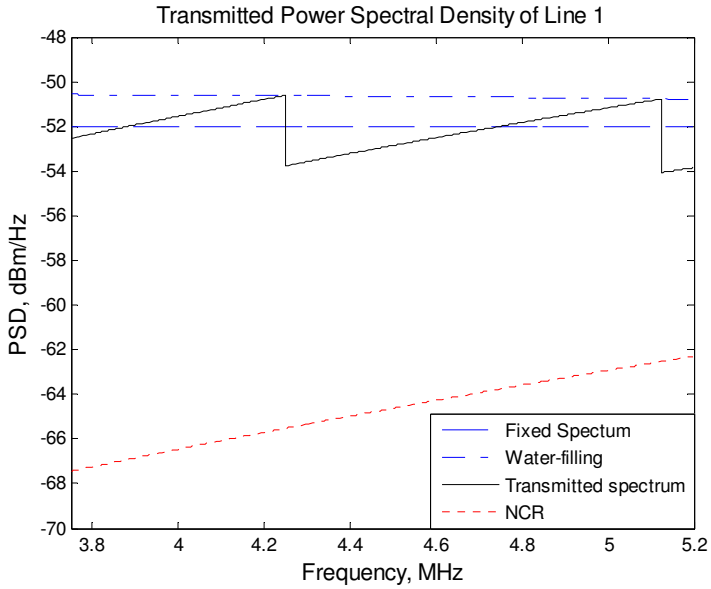

Figure 24: PSD in L_1 with two interferers

L_2 and L_3 contribute with interference from a fixed transmitted spectrum at nominal value.

The rates of the two short lines were constrained to the bit rate at fixed spectrum at; R = 13.63 Mbps and the iterative water-filling algorithm was performed on the system. As in Chapter 3.4 the water-filling was first performed to the second line while assuming a fixed transmitted spectrum at nominal value in both interfering lines, i.e. $S_1(f) = S_3(f) = S_0$. Successive water-filling was performed in L_3 with calculated interference from the adjusted PSD in L_2 and assumptions of the interference from L_1, i.e. $S_1(f) = S_0$. The subsequent water-filling of L_1 calculates however precisely both the interference from L_2 and L_3. The water-filling of L_2 will now similarly be based on accurate calculations and so forth. Table 4 presents the bit rates after running ten iterations of the water-filling algorithm in each subscriber line.

Table 4: Bit rates of three active lines after IWF

	L_1	L_2	L_3
Fixed Spectrum	5.48 Mbps	13.63 Mbps	13.63 Mbps
Iterative Water-filling	10.91 Mbps	13.79 Mbps	13.73 Mbps

By increasing the permitted bit rates in the disturbing lines; a rate region of the three subscribers can be presented as in the two-user environment in Chapter 3.4. A rate region of three lines is however less comprehensible and both the capacity for L_2 and L_3 are illustrated in the horizontal axis in Figure 25. The two sets of bit rate pairs are however nearly identical, as seen in the illustration, differing only based on the order in which they are water-filled, i.e. L_2 is water-filled prior to the water-filling of L_3.

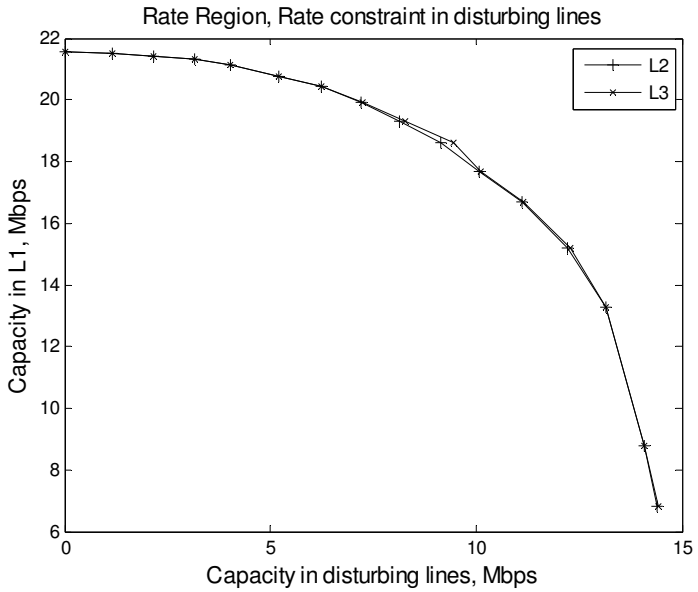

Figure 25: Rate region with three active lines

The rate region shows the decreasing bit rate in L_1 as a result of the increasing bit rates in the disturbers.

3.8.3. PSD Constraint

As seen in the previous section's iterative water-filling the interference from two short lines represents a significant increase in the interference compared to the interference experienced by the long line in the two-user environment of Chapter 3.6. None the less, two disturbers of line length 500 meters interfere with too little crosstalk to activate the PSD constraint. Thus the lengths of the interfering twisted pairs are once more shortened to 100 meters, as illustrated in Figure 26:

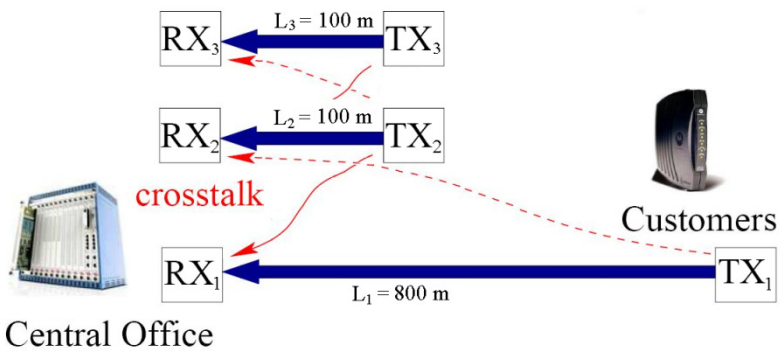

Figure 26: Two dominant interferers

When two equally dominating interferers are present in a system, these subscriber lines will also create a significant disturbance to each other and thus not be able to apply the same PBO as in a two-user environment. The transmitted spectrum in L_1 after water-filling and its dominating NCR are illustrated in Figure 27:

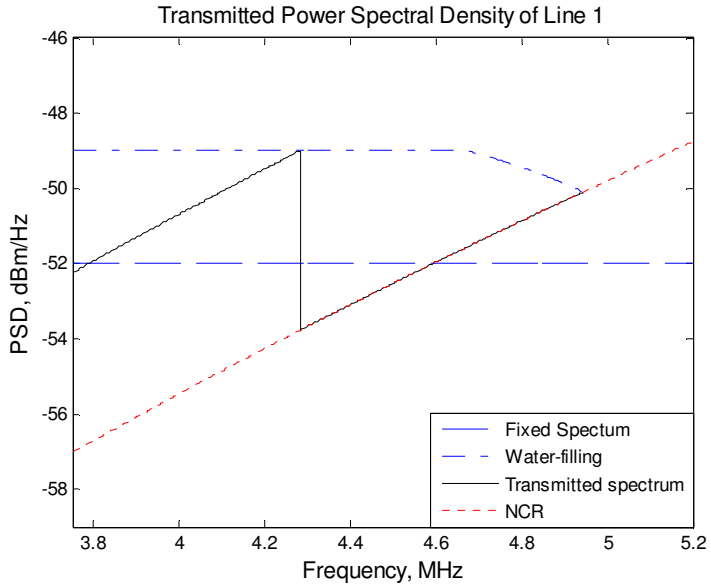

Figure 27: PSD constraint in three-user environment

The figure illustrates a severely constrained PSD for line 1 with two powerful disturbers.

The water-filling and consequently the transmitted spectrum are evidently constrained to -49 dBm/Hz, as specified in (29). The NCR exceeds the water-filling graph for the highest frequencies and these carriers are thus shut off, i.e. $S_1(f) = 0$. The iterative water-filling algorithm continues with the water-filling of L_2 which assumes a fixed spectrum at nominal value for L_3. Even though the interference from L_3 at nominal value is significant, the short attenuation leads to redundant power to achieve its required bit rate, consequently introducing PBO to its transmitted spectrum. Hence L_3 will experience less interference than if a fixed spectrum was present in L_2, and will thus apply an even greater PBO than the PBO applied to L_2. The successive water-filling of L_1 will thus be based on accurate calculations of the

interfering crosstalk with both disturbers applying PBO. Figure 28 presents the transmitted PSD of L_1 after the water-filling algorithm is applied to its disturbers.

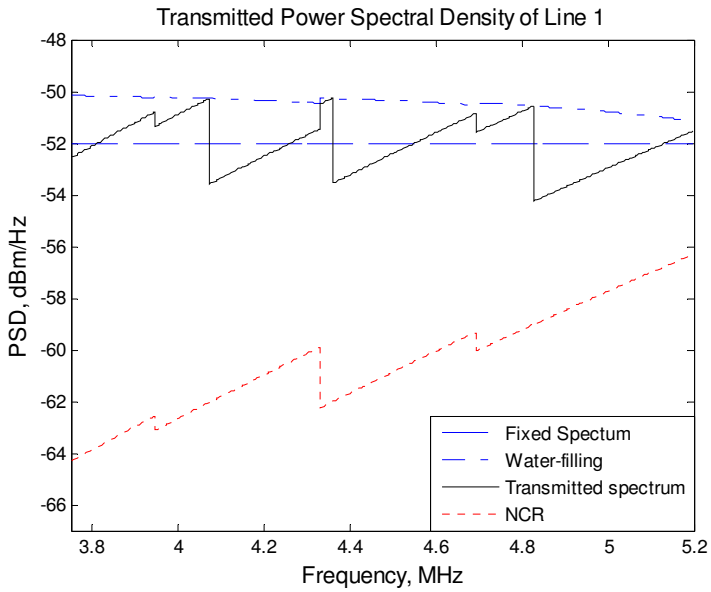

Figure 28: PSD constraint in three-user environment II

Line 1 has now spread its spectrum to all carriers eliminating the need of a PSD constraint.

The big *step* in L_1's NCR around 4.3 MHz corresponds to a peak in the transmitted PSD of the strongest interferer with the least applied PBO; namely L_2, whiles the smaller steps at ~ 3.95 MHz and ~ 4.7 MHz correspond to peaks in the PSD of the weaker disturber, L_3. The PSD is clearly lower than the PSD constraint in every carrier. A rate region of these three subscriber lines' bit rate pairs is presented in Figure 29.

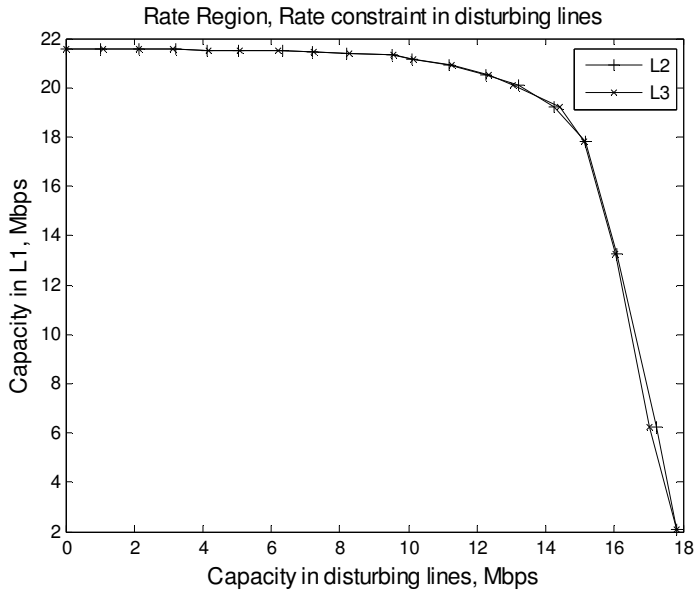

Figure 29: Rate region with three active lines II

The illustration presents the rate region of a L_1 at 800 meters vs. two powerful disturbers at 100 meters.

3.9.Differences in the Crosstalk Coupling

In the previous chapters; calculations has been performed with either a two-user environment and thus only one crosstalk coupling, or with a fixed coupling coefficient for all coupling relations in a three-user environment. In the following calculations a fixed crosstalk coefficient equivalent to (17) was applied to the pair-to-pair coupling as follows:

$$K_{FEXT}(1,2) = -45 \text{ dBm/km/Hz} \quad (38)$$

$$K_{FEXT}(1,3) = -48 \text{ dBm/km/Hz} \quad (39)$$

$$K_{FEXT}(2,3) = -45 \text{ dBm/km/Hz} \quad (40)$$

The crosstalk coefficient describes the coupling relation between two lines and is thus symmetrical, i.e. $K_{FEXT}(i,j) = K_{FEXT}(j,i)$. The subscriber line lengths of 800 meters for L_1 and 500 meters for L_2 and L_3, as in Chapter 3.8, were again chosen for uncomplicated comparison with previous results. Static spectrum management resulted in bit rates of; R_1 = 6.18 Mbps, R_2 = 13.63 Mbps and R_3 = 13.67 Mbps while the iterative water-filling with 10 iterations achieved bit rates of; R_1 = 10.03 Mbps, R_2 = 13.71 Mbps and R_3 = 13.83 Mbps.

3.10. Ten Active Pairs

A statistical model of the probability distributions of FEXT power sum is presented by Holte [2] with references to measurements of crosstalk in each individual pair-to-pair combination. A matrix of the expected crosstalk coupling based on these measurements is presented in Table 5.

Table 5: FEXT coupling matrix

The table presents the pair-to-pair crosstalk coupling in a full 10-pair binder.

	46,1	50,2	52,4	53,9	54,6	54,4	55,3	53,2	50,8
46,1		48,0	49,9	52,4	54,6	54,3	53,1	51,2	50,4
50,2	48,0		47,5	51,2	53,8	54,8	50,0	49,5	53,0
52,4	49,9	47,5		47,3	50,8	50,4	49,7	54,2	55,2
53,9	52,4	51,2	47,3		46,3	49,0	51,6	54,5	54,0
54,6	54,6	53,8	50,8	46,3		47,3	51,4	54,3	55,1
54,4	54,3	54,8	50,4	49,0	47,3		47,7	52,1	53,5
55,3	53,1	50,0	49,7	51,6	51,4	47,7		47,5	50,5
53,2	51,2	49,5	54,2	54,5	54,3	52,1	47,5		47,3
50,8	50,4	53,0	55,2	54,0	55,1	53,5	50,5	47,3	

In these calculations a statistical FEXT coupling was derived as the product of the coupling coefficient matrix and a Gaussian distributed variable given in (41).

$$X = N(0,1) \tag{41}$$

Hence, the variable has zero expectancy and unit standard deviation. The crosstalk pair-to-pair coefficient of pair *i* and pair *j* was then given by the following expression:

$$K_{FEXT}(i,j) = E[X_{FE}(i,j)] \cdot X^2 \tag{42}$$

$E[X_{FE}(i,j)]$ is the expected crosstalk coupling given in Table 5. The binder for the calculations presented in this chapter consists of ten active lines where L_1 is 800 meters and the other lines are 500 meters. For comparison the system is initially calculated with the same crosstalk coefficient of; $K_{FEXT}(i,j) = -45$ dBm/km/Hz, as given in (17). The bit rates of the system with a fixed spectrum at nominal value are presented in the first column in Table 6. By adjusting the crosstalk coupling coefficient as expressed in (42) a new set of bit rates was achieved and presented in the second column of Table 6. The Gaussian distributed variable X varies for all calculations and could cause big variations to the capacities. Hence, it has to be taken into consideration when comparing the capacities. Similar calculations were performed for a dynamic spectrum by the iterative water-filling algorithm, initially with a nominal FEXT coupling coefficient and secondly with statistical FEXT coupling based on the same variable X as in the previous calculation. A rate constraint, equal the values at SSM presented in the second column of Table 6, was applied to the interfering subscriber lines. No constraint was however applied to L_1's bit rate since the objective was to maximize this bit rate. The resulting capacities are presented in the third column of Table 6 for the case with fixed crosstalk coupling and in the fourth column for the case with statistical crosstalk coupling.

Table 6: Capacities for ten active subscriber lines

The table presents the capacity in each line with fixed and statistical crosstalk for both SSM and Water-Filling. The Gaussian distributed variable is given as *X* in the statistical calculations. All rates are given in Mbps.

	SSM		Water-Filling	
	Fixed Crosstalk	Statistical X = 0.6355	Fixed Crosstalk	Statistical X = 0.6355
L_1	2,70	7,25	5,26	11,11
L_2	9,38	14,29	9,95	14,60
L_3	9,38	13,81	9,98	14,01
L_4	9,38	13,62	9,95	13,70
L_5	9,38	13,60	9,89	13,69
L_6	9,38	13,90	9,88	14,36
L_7	9,38	13,81	9,87	14,17
L_8	9,38	13,58	9,88	13,71
L_9	9,38	13,89	9,88	13,93
L_{10}	9,38	14,50	9,94	14,52

4. DISCUSSION

In this chapter the results from Chapter 3 will be evaluated and discussed. This includes any figures presenting obtained results which will be discussed with a reference to the figure in the mentioned chapter. The different algorithms and calculations will be discussed in the same order they were presented in Chapter 3.

4.1. Fixed Spectrum

4.1.1. Full power on two active lines

The implemented algorithm returned a bit rate of; $R_2 = 20.30$ Mbps for the shortest line while the longer line, L_1, only achieved a bit rate of; $R_1 = 6.87$ Mbps. Comparing these rates to bit rates at crosstalk independent lines at $R_2 = 21.75$ Mbps and $R_1 = 20.92$ Mbps, exhibit the longer line has a decisive interference from the shorter line, while it appears L_2 hardly is interfered by crosstalk coupling at all. However, when L_2 is crosstalk independent the limiting factor is not the attenuation but the bandwidth efficiency maximum (BWEM). Operating with higher bandwidth efficiencies, if possible, would result in a bit rate of; $R_2 = 27.90$ Mbps; a significant increase compared to the bit rate when crosstalk from L_1 was included. L_2 is thus undeniably affected by crosstalk but it is however not a decisive impairment as experienced for the longest line.

4.1.2. Introducing Power Back-Off

Accepting a small reduction in the capacity for the shortest line with a PBO of 11.1 dB increases the capacity of L_1 to 12.23 Mbps; an increase of 78 percent. The capacity in L_2 is now reduced to 15.05 Mbps or a decrease of less than 26 percent. Distributing less power for the shortest line permits a higher capacity for the longer line, resulting in a more balanced distributed capacity from a slightly greater overall capacity, as illustrated in Figure 30.

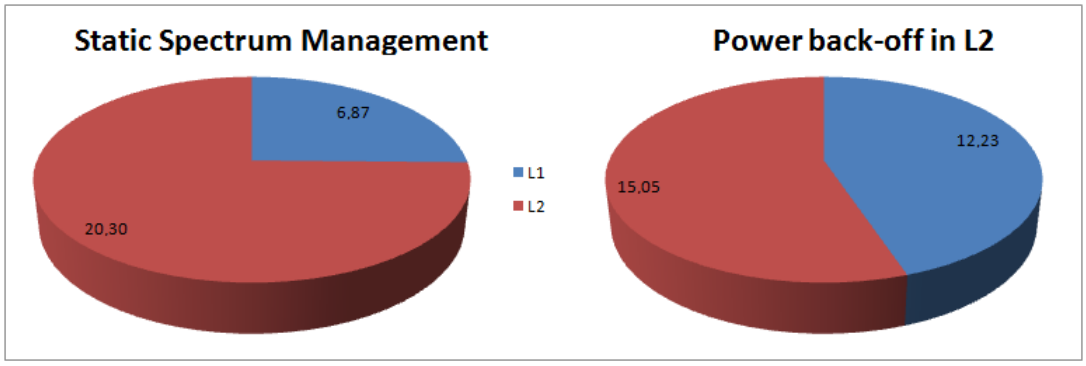

Figure 30: Bit rate distribution

The figure illustrates how a decrease in capacity in a twisted pair leads to an increase in the capacity of an adjacent twisted pair in the same binder.

4.1.3. Presenting the Rate Region

In addition to power back-off; also boosting was permitted in the transmitted spectrum of the shortest line. This was as mentioned only for illustration since boosting on the shortest line would result in only a small gain in the shortest line's bit rate, but a significant increase in the emanating crosstalk. If an increase in the shortest line was desirable an applied PBO to the longest line would possibly have been a better alternative. This was however not applied in the system based on inconvenience when presenting the rate region.

4.2. Single-bit Bit Loading

The returned bit rate of; $R_1 = 7.61$ Mbps after bit loading is equivalent to an increase of 10.8 percent compared to the bit rate with static spectrum management. This increase in capacity comes merely from shifting the spectrum density, an algorithm which easily could be adapted to existing modems. Calculations of the bit rate in a system with 11.1 dB PBO resulted in only a 5.2 percent increase compared to the bit rate at static spectrum management. Hence, the iterative bit loading is considerably more efficient at lower bit rates, increasing the bandwidth efficiency with an average of half a bit/s independently of the calculated system.

4.3. Water-Filling

When applied to the initial system of $L_1 = 800$ meters and $L_2 = 500$ meters with power back-off; PBO = 11.1 dB the water-filling algorithm resulted in a bit rate for the longest line of $R_1 = 12.87$ Mbps while maintaining a bit rate in the shortest line of; $R_2 = 15$ Mbps. Bit loading with the same PBO achieved the exact same bit rate, thus water-filling achieves no capacity advantage. Comparing the power allocations of the algorithms evidently reveal both algorithms achieve identical transmit power spectral densities. The bit loading algorithm presented in Chapter 3.2 is thus in fact also the power allocation of the water-filling algorithm, although applied in a more straight forward approach. Furthermore the noise-to-channel ratio in Figure 11 is too weak to make a real impact on the power allocation compared to a fixed spectrum thus the water-filling line is nearly flat, i.e. the basis for the power allocation is frequency independent. The only gain of the algorithm is achieved by shifting the transmit spectrum from carriers where no integer number of bits can be loaded. Thus the bit allocation equals the bit allocation at static spectrum management when a fixed PSD equal the water-filling basis is applied. This would however significantly increase the transmit power. A fictitious penalty was then applied to the longest line's signal-to-noise ratio to illustrate the water-filling better. Figure 12 illustrates significant PSD variations in the

water-filling due to the frequency dependency in the dominant NCR. Carriers in the lower frequency band receive a higher power spectral density than the other carriers, consequently increasing their bit allocation. The resulting bit rates demonstrated a significant increase of 37 percent compared to the static spectrum approach of Chapter 3.1.2.

4.4. Iterative Water-Filling

The iterative water-filling executes the water-filling algorithm iteratively on the twisted pairs in the system. The IWF algorithm of Chapter 3.4 was implemented with the objective to maximize the bit rate of the long line; L_1, while applying a rate constraint to the shorter line; L_2. When constraining the bit rate of L_2 to the rate of a transmit spectrum at nominal value applied a flat PBO of 11.1 dB, the water-filling algorithm reduced the power allocation in all carriers, simultaneously reducing the interference of all carriers in L_1. The transmitted power in L_2 was reduced to less than 6 percent of the power at nominal spectrum and by a margin of 30 percent compared to the power at fixed spectrum with 11.1 dB power back-off. As the dominant impairment of L_1 this leads to a significant increase in this subscriber's bit rate, given by executing the water-filling algorithm in L_1. Every iteration of the iterative water-filling resulted in a new set of crosstalk interference, however the bit rate quickly stabilized and after 5 iterations of water-filling in each line the bit rate achieved a gain of 0.92 Mbps compared to the bit rate with a fixed transmit spectrum in the interfering line. The crosstalk interference from the dominating line is significantly reduced, without any reductions to the capacity of this line.

4.5. Great Differences in Cable Length

The initial system with twisted pair lengths of 500 meters and 800 meters have been presented to have too little interfering crosstalk to illustrate water-filling in the most comprehensive way. The length of the shortest twisted pair was thus reduced first to 300 meters, and then to a diminutive 100 meters. Figure 17, and in particular the right figure illustrating the transmit spectrum in a linear presentation, illustrated significant frequency dependency in the transmitted spectrum. The transmitted bit rate of; $R_1 = 4.35$ Mbps, in the initial system introduced a significant gain compared to the bit rate at static spectrum management of; $R_{SSM} = 3.66$ Mbps. At twisted pair lengths of 800 and 100 meters, the interference even leads to spectrum nulls in the transmitted PSD for the highest frequencies as presented in Figure 31, presented both in logarithmic and linear scale. The transmitted spectrum is dominated by the interfering crosstalk and the significant attenuation, thus the signal-to-noise ratio falls below

unity. Neither at fixed spectrum nor at water-filling can bit loading occur with SNR below unity. However, in contradiction to SSM, the water-filling algorithm will shut these tones off and let the spare power be used in other frequencies, thus not wasting any power at interference dominated tones. This is arguably the biggest advantage of dynamic spectrum management. The resulting bit rate is only 2.59 Mbps, but compared to static spectrum management; water-filling has achieved a 34 percent increase.

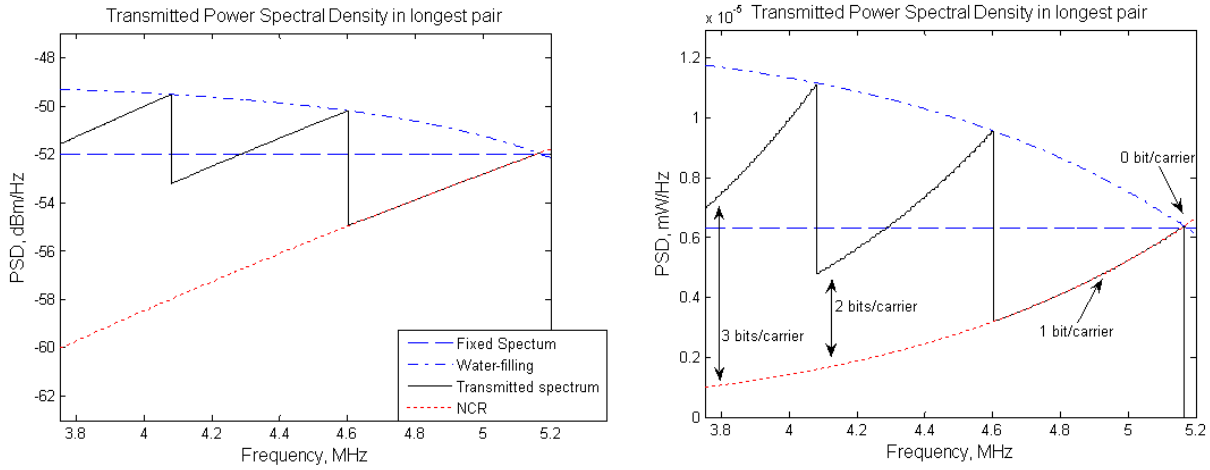

Figure 31: Water-filling with decisive interference

Both figures now clearly show how water-filling increases the spectrum at lower values of NCR which in this case is so severe it causes nulls in the transmitted spectrum; the highest frequencies are shut off.

4.6. PSD Constraint

A constraint was applied to the power spectral density to prohibit peaks in the transmitted spectrum. However, even with the decisive interference of Chapter 3.5 with pair lengths of 800 and 100 meters the PSD does not reach these levels, illustrated by a PSD still within the conditions of the constraint in Figure 31. The PSD constraint will affect the spectrum only with an increase in the attenuation or the presence of even more powerful interference. The interference could be caused by the introduction of interfering subscribers even closer to the CO or from additional active pairs in the binder. The shortest pair was however already minimal and three active pairs was not presented until Chapter 3.7. Consequently, the attenuation was made more decisive by increasing the length of the longest line to 900 meters. When applying the constraint to this system in a straight forward approach, calculations of the transmitted power verified the transmit power had been reduced by a third compared to the available power. When the objective is bit rate maximization; transmitting just two thirds of the available power is obviously inadequate. Hence the straight forward approach was disposed of for this purpose. The second approach, presented in the right illustration of Figure 18, evidently reached the PSD constraint for every carriers not being shut off, i.e. all carriers

possibly adding a bit without exceeding the PSD constraint have done so and the water-filling graph is presented by a flat line. Nor here was the upper limit for the total power reached, although it came within 5 percent of the available power. It also obtained a 5 percent reduction to its bit rate compared to the case without a PSD constraint. Adjusting the length of the shortest pair to a distance of 200 meters decreased the interference which resulted in less NCR and consequently allowed a full power usage without exceeding the constraint, illustrated by Figure 19. The two cases, with and without a PSD constraint, now resulted in approximately the same bit rate with a slight favour to the case with no constraint. Evidently there is little variation to the bit rate although the transmitted spectrums are noticeably different. The PSD constraint is as mentioned only necessary in cases with extensive attenuation or interference. In the case of upstream communication, this kind of interference will only exist for disturbing transmitters in close proximity to the CO. In the two line perspective, DSM will in reality apply power back-off to these short lines and thus eliminate the overwhelming crosstalk alongside the need for a constrained PSD. In binders with more than two active users the case may be different, as was investigated in Chapter 3.8.

4.7. Top-Filling

The top-filling algorithm was applied to the interfering line; L_2, which consequently led to interference free carriers for the lowest frequencies in L_1. Figure 21 illustrated however that less than 20 percent of the transmitted power was allocated in these bands. Hence, more than 80 percent of the permitted power was transmitted in interference dominated frequency bands in futile attempts to increase the bit rate. The water-filling of L_1 with a static spectrum in a similar, interfering line was simulated in Chapter 3.3 and returned a bit rate of 12.84 Mbps, 1.25 Mbps higher than what was achieved with a top-filled interfering subscriber line. The linear rate region presented in Figure 22 also illustrated the less attractive bit rates at top-filling compared to the rate region of the iterative water-filling algorithm in Figure 15. Consequently, the top-filling algorithm was not included in any further calculations.

4.8. Three Active Pairs

4.8.1. Fixed Spectrum

The implementation of a three-user environment was performed in Chapter 3.8 where calculations of the bit rates were performed with static transmit spectrums in all three lines. The returned bit rates were; $R_1 = 5.48$ Mbps for the long line and; $R = 13.63$ Mbps for both shorter lines. These two shorter lines were operated under identical conditions and naturally

obtained equal bit rates. The introduction of a third twisted pair introduces a significant increase in the interference for the longest line and thus also a reduction to the bit rate compared with the bit rate in a two-user case of; R_1 = 6.87 Mbps, as presented in Chapter 3.1.1. This is however a small reduction compared to the reduction in L_2 which previously obtained a bit rate of; R_2 = 20.3 Mbps. This line experienced little crosstalk from L_1 in the two-user environment, but has now gained a significant interferer in L_3 and has had its capacity reduced by nearly a third.

4.8.2. Water-filling

Successively, water-filling was performed for the three-user environment resulting in similar reductions as for the static spectrum management. More interesting however were the results obtained from iterative water-filling: By limiting the rate in the two short lines to the rate at fixed spectrum at 13.63 Mbps, the interference reduction in L_1 is twice as big as for the case with only two active lines. Thus the increase in capacity is also significantly higher than what was presented for the two-user case in Chapter 3.4. Figure 32 below presents the bit rates after iterative water-filling corresponding to Table 4 in Chapter 3.8.2. The resulting bit rate in L_1 was calculated to twice the value of the bit rate at static spectrum management.

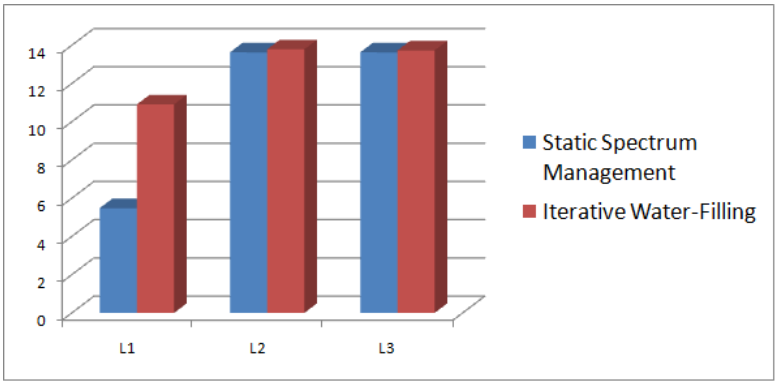

Figure 32: Bit rates of three active lines

The figure presents the bit rates in Mbps with fixed spectrum and after iterative water-filling.

The rate region presented in Figure 25 illustrates that the two disturbing subscriber lines of equal cable length observe similar but not identical bit rates, even though both L_2 and L_3 have the same applied bit rate constraints. However, the water-filling algorithm, as implemented in this thesis, cannot meet the bit rate constraints exactly. Furthermore, since L_2 is water-filled prior to L_3 the first water-filling of L_2 will assume a fixed spectrum in L_3. In contradiction the first water-filling of L_3 will be based on the water-filling of L_2 evidently creating small differences visible in the rate region.

4.8.3. PSD Constraint

The introduction of power back-off to the dominating lines of L2 and L3 in the iterative water-filling algorithm evidently reduced the transmit spectrums of both lines significantly. Figure 28 illustrated the spectrum was spread across the entire bandwidth with the most significant spectral component again well below the PSD constraint, hence eliminating the need of a PSD constraint once again.

4.9.Differences in the Crosstalk Coupling

The 3 dB reduction in the crosstalk coupling between L_1 and L_3 led to a notable increase in the longest line's bit rate of 13 percent compared to the bit rate at static spectrum management of 5.48 Mbps, calculated in Chapter 3.8.1. The capacity of L_2 unsurprisingly stayed the same as both $K_{FEXT}(1,2)$ and $K_{FEXT}(3,2)$ still have the same crosstalk coupling as it had in the previous calculations. L_3 achieved a slight increase to its bit rate due to less interference from L_1. The contribution was however a mere 0.32 percent since the coupling to the dominant interferer in L_2 was unaffected. The iterative water-filling also illustrated a slight increase to the bit rate in L_1. This increase would possibly have been higher if the rates of the interfering lines more accurately met the bit rate constraint given by the bit rates at static spectrum management of; R2 = 13.67 Mbps and R3 = 13.67 Mbps, instead of notably surpassing them. Implementing a more accurate constraint would however significantly increase the complexity of the algorithm. An accurate constraint would also be achieved by performing single-bit bit loading on the interfering lines though this would delay convergence. Neither the single-bit bit loading nor any other more accurate algorithms were implemented for these calculations.

4.10. Ten Active Pairs

The crosstalk coupling of a 10-pair binder gets more difficult to predict as the number of active pairs increases. Calculations prior to Chapter 3.9 applied a fixed coupling coefficient for all pair-to-pair combinations independent of the locations of the twisted pairs in the binder. The coupling relations are in reality distinct for all disturbers based on many different parameters, e.g. location in the cable and proximity to the coupled pair. The coupling matrix presented in Table 5 illustrates a powerful crosstalk between adjacent twisted pairs. L_1 will consequently experience greater interference from line L_2, L_3 and L_9 compared with L_5, L_6 and L_7. This is illustrated in the resulting bit rates in the second- and forth columns of Table 6 where L_2 and L_9 evidently reach higher bit rates. Both these lines would have experienced L_1

as one of their main interferers, as seen in Table 5, and thus receive a greater reduction in interference since L_1's signals are attenuated prior to interfering on the other lines. When the subscriber lines are water-filled however, all lines except L_1 approximate a rate constraint which would eliminate this difference. Hence, the rate constraint of the water-filling algorithm was set equal to the bit rates at SSM in the second column of Table 6, thus the bit rates of the twisted pairs after water-filling differ to each other similarly as at SSM. This is solely to compare the bit rate in L_1 at SSM to the bit rate in L_1 after water-filling in the best possible way and the rate constraint can easily be adjusted to a fixed value for all lines. Given a different Gaussian distributed variable X, the resulting bit rates presented in Table 6 would be significantly altered. However, the difference in capacity of the crosstalk impaired line at SSM compared to after iterative water-filling is significant, as illustrated in Figure 33. Consequently, the fixed crosstalk coupling coefficient of; K_{FEXT} = -45 dBm/km/Hz, is a severely pessimistic assumption when the binder consists of 10 active pairs. Moreover, the water-filling algorithm seems to have lost some of its advantage when the binder is full, offering an increase of 53 percent to the subscriber furthest away compared to an increase of 99 percent come to the three-user environment. The resulting bit rates at static spectrum management and after water-filling corresponding to respectively the second and fourth columns of Table 6, both applied statistical crosstalk coupling, are presented in Figure 33.

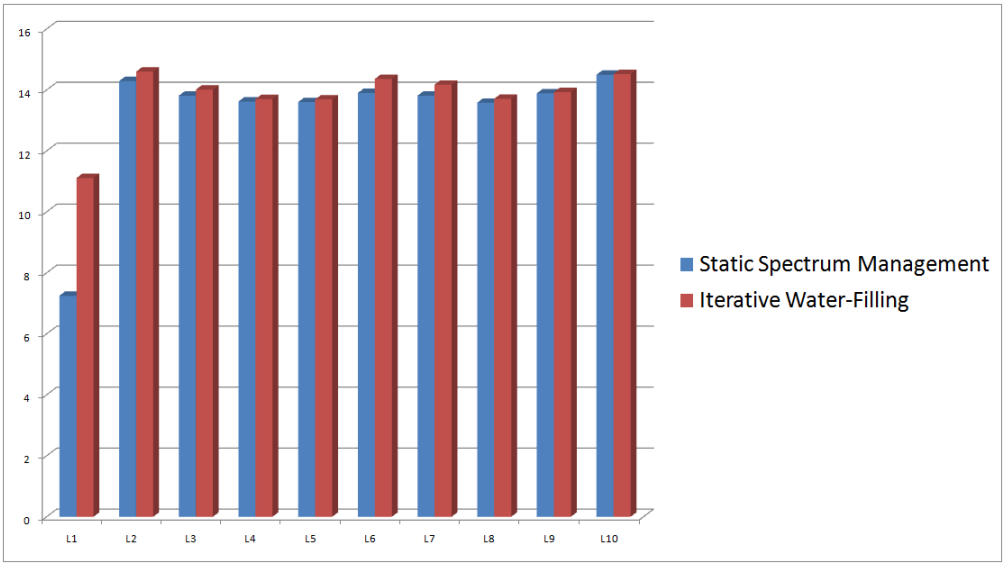

Figure 33: Bit rates of ten active lines

The figure presents the bit rates in Mbps at static spectrum management and after iterative water-filling.

5. CONCLUSION

Crosstalk coupling is the impairing interference in present digital subscriber lines. The algorithms presented herein evidently demonstrate there are significant improvements to achieve from autonomous algorithms for dynamic power allocation. Dynamic Spectrum Management, and in this thesis in particular the iterative water-filling algorithm, contributes with significant crosstalk reduction between subscriber lines. Implementing these algorithms in user terminals in last mile, twisted pair communication would increase bit rates and still preserve compatibility with existing equipment. However, existing modems based on worst case crosstalk assumptions would significantly reduce the potential gain. The efficiency of implementing DSM in the terminals will thus increase proportional to the number of terminals implementing the algorithm. Even though fibre to the home could offer even greater bit rates it is not an economical equivalent hitherto as DSM offers implementation with mere software upgrades and thus limited financial investments. Implementation of autonomous algorithms in present communication systems consequently imply DSL would gain an even greater advantage over other broadband communication technologies until more advanced algorithms at DSM level two and three are ready to lead DSL even further.

Bibliography

1. **Holte, Nils.** Broadband communication in existing communication cables by means of xDSL systems - a tutorial. *Proceedings from NORSIG-2001.* Trondheim 18-20 oct. 2001.

2. **Holte, Nils.** An analytical model for the probability distributions of crosstalk power sum for a subset of pairs in a twisted pair cable. *Global Telecommunication Conference, 2004. GLOBECOM '04. IEEE.* 313-317 Vol.1, 2004.

3. **Cendrillion, R., et al.** Autonomous Spectrum Balancing for Digital Subscriber Lines. *IEEE Transaction on Signal Processing.* Volume: 55, Issue: 8, Aug. 2007, pp 4241-4257.

4. **Schelstraete, S.** Defining upstream power backoff for VDSL. *IEEE Journal on Selected Areas in Communications.* Volume 20, Issue 5, Jun 2002, pp 1064 - 1074.

5. **Unger, J. H.W.** *Near-end crosstalk model for line code studies.* ANSI T1D1.3/85-244, Nov. 1985.

6. **Haykin, S.** *Communication Systems 4th edition.* Hoboken, NJ : John Wiley & Sons, 2001.

7. **Clarke, D., et al.** A new analytical method for NEXT and FEXT noise calculation. *T1E1.4-189, ANSI T1E1.4 meeting in Huntsville, AL.* June 1998.

8. **Cook, J., Magnone, L. and Persico, R.** *Proposed working text for appendix, Crosstalk combination.* T1E1.4/99-175, Arlington (VA), April 20-23, 1999.

9. *DSL Spectrum Management.* **Huang, J.** Guest Lecture of ELE539A Princeton University, March 2007 (url: http://www.princeton.edu/~chiangm/ele539l12.pdf). 10. **ITU-T G.992.1.** *Asymmetrical Digital Subscriber Line (ADSL) transceivers.* Telecommunication Standardization Sector of ITU, 1999.

11. **Verlinden, J., et al.** Protecting The Robustness Of ADSL And VDSL DMT Modems When Applying DSM. *In International Zurich Seminar on Communications.* Switzerland, Feb. 2004.

12. **Bogaert, E. Van den, et al.** DSM in Practice: Performance Results of Iterative Water-filling Implemented on ADSL Modems. *IEEE International Conference on Acoustics, Speech and Signal Processing (ICASSP).* May 2004, pp. 337-340.

13. **Golden, P., Dedieu, H. and Jacobsen, K. S.** *Fundamentals of DSL Technology.* Boca Raton, FL : Auerbach Publications, 2005.

14. **Yu, W., Ginis, G. and Cioffi, J. M.** Distributed multiuser power control for digital subscriber lines. *IEEE Journal on Selected Areas in Communication.* Volume: 20, Issue: 5, June 2002, pp 1105-1115.

15. **Cendrillion, R., et al.** A Near-Optimal Linear Crosstalk Canceler for Upstream VDSL. *IEEE Transactions on Signal Processing.* Volume: 54, Issue 8, Aug. 2006, pp 3136 - 3146.

16. **Cioffi, J. M., et al.** *DSM Level 1: Polite Low-Power Single-DSL Stability.* NIPP-NAI-2007-158R1.

17. *DSL Broadband: 1000M x 1000M.* **Cioffi, J. M.** Presentasjon ved Stanford University, 2004.

18. **Cioffi, J. M. and Mohseni, M.** Dynamic Spectrum Management - A methodology for providing significantly higher broadband capacity to the users. *Telenor Telektronikk Journal on Telecommunication Forecasting.* Volume: 4, 2004, pp 123-137.

19. **Golden, P., Dedieu, H. and Jacobsen, K. S.** *Implementation and Applications of DSL Technology.* Boca Raton, FL : CRC Press, 2007.

20. **Cendrillion, R., et al.** Optimal multiuser spectrum balancing for digital subscriber lines. *IEEE Transactions on Communications.* Volume: 55, Issue: 8, Aug. 2007, pp 4241-4257.

21. **Cioffi, John M, et al.** Vectored DSLs with DSM: The road to ubiquitous Gigabit DSLs. *Proc. IEEE World Telecommunication Congress in Budapest, Hungary.* 2006.

22. **Starr, T., et al.** *DSL Advances.* Upper Saddle River, NJ : Prentice Hall, 2002.

23. **Song, K. B., et al.** Dynamic Spectrum Management for Next-Generation DSL Systems. *IEEE Communications Magazine.* Volume: 40, Issue: 10, Oct. 2002, pp 101- 109.

24. *A Dual Decomposition Approach to the Sum Power Gaussian VEctor Multiple Access Channel Sum Capacity Problem.* **Yu, Wei.** The John Hopkins University : 2003 Conference on Information Sciences and Systems, March 12-14, 2003.

25. **ANSI-T1.417.** *Spectrum management for loop transmission systems.* Issue 2, ANSI, Nov. 2002.

26. **Fudenberg, D and Tirole, J.** *Game Theory.* MA : MIT Press, Aug. 1991.

27. **ITU-T G.993.1.** *Very high speed digital subscriber line transceivers.* Telecommunication Standardization Sector of ITU, 2004. Annex A.

28. **Dris, Stefanos, et al.** Maximizing the Bandwidth Efficiency of the CMS Tracker Analog Optical Links. *Hedielberg 2005, Electronics for LHC and future experimnets.* Nov. 2005.

29. **Andgart, Niklas, et al.** PSD-Constrained PAR Reduction for DMT/OFDM. *EURASIP Journal on Applied Signal Processing.* 2004:10, 1498-1507, 2004.

APPENDIX A: *README* FOR MATLAB® PROGRAMS

All programs developed for the calculations in this thesis have been submitted when submitting the thesis for censorship and can be made available through NTNU's digital archives for submitted master thesis (DAIM).

The submitted MATLAB® programs:

bitload.m	Single-bit bit loading
defVDSLu.m	Default input data for VDSL calculations
FEgen.m	Matrix corresponding to Table 5
fext.m	Model for calculating the FEXT
initial.m	Initialize data from VDSL calculations
itwaterfill.m	Iterative water-filling algorithm
itwaterfillfast.m	IWF with no presentations for faster performance in other programs
itwaterfillRR.m	Presenting rate region based on IWF
plotcaps.m	Presenting capacity with two static lines
sig.m	Initialize signal power
singcap.m	Calculate capacity
sys.m	Defining the system and calculate system parameters
topfill.m	Top-filling algorithm
topfillfast.m	TF with no presentations for faster performance in other programs
waterfill.m	Calculates the water-filled spectrum
waterfillfast.m	WF with no presentations for faster performance in other programs
whnoi.m	Initialize white noise